Project Report

CMP-19

M.L. Meeks

VHF Propagation Over Hilly, Forested Terrain

9 April 1982

Prepared for the Defense Advanced Research Projects Agency
under Electronic Systems Division Contract F19628-80-C-0002 by

Lincoln Laboratory

MASSACHUSETTS INSTITUTE OF TECHNOLOGY

LEXINGTON, MASSACHUSETTS

The work reported in this document was performed at Lincoln Laboratory, a center for research operated by Massachusetts Institute of Technology. This work was sponsored by the Defense Advanced Research Projects Agency under Air Force Contract F19628-90-C-0002 (ARPA Order 5724).

MASSACHUSETTS INSTITUTE OF TECHNOLOGY
LINCOLN LABORATORY

VHF PROPAGATION OVER HILLY FORESTED TERRAIN

M.I. MEEKS
Group 48

PROJECT REPORT CMT-19

9 APRIL 1982

LEXINGTON MASSACHUSETTS

ABSTRACT

We have made propagation measurements at low altitudes over hilly, forested terrain with the objective of developing a computer-based propagation model capable of predicting path loss given the terrain profile between transmitter and receiver. The measurements were made at a frequency of 110.6 MHz with the VOR station at Gardner, Massachusetts, as a transmitter. The received signal was measured at distances between 7 and 15 km by making vertical descents with a helicopter from altitudes of roughly 800 m down to 10 m above ground. We found good agreement between the measurements and model predictions based on an extension of the Deygout approximation. Use of two knife-edges was sufficient to characterize the terrain diffraction. Negligible multipath reflection was observed from this terrain.

CONTENTS

List of Illustrations

List of Tables

1. Introduction

We have made VHF propagation measurements at low altitudes over hilly, forested terrain with the objective of developing a computer-based propagation model capable of predicting path loss given the terrain profile between the transmitter and receiver. As a transmitter for these measurements we used an aircraft-navigation aid, a VOR (for VHF Omnidirectional Range) station* located near Gardner, Massachusetts. We used a helicopter to probe the signal strength as a function of height at six locations between 6.6 and 15.3 km from the transmitter. Since our objective was to develop a propagation model, we selected paths for measurement that presented modeling difficulties because of multiple diffraction or the lack of clearance of the first Fresnel zone.

We tested various modeling assumptions against the measured data to determine the appropriate algorithm for automatically selecting edges on the terrain profiles. By measuring the path intersections with contours on large-scale maps, we obtained accurate terrain profiles; we also used profile data derived from digital terrain-relief maps provided by the Defense Mapping Agency (DMA). Appendix A compares the profiles obtained by these two methods and presents propagation

*The nationwide network of VOR stations operating in the frequency range 108 to 118 MHz provides well sited, ground-based transmitters that can be used for propagation measurements. A wide variety of terrain types could be investigated by selecting appropriate VOR sites.

predictions for the DMA profiles. We also compared the predictions of our propagation model with those of the Longley-Rice model (Longley & Rice, 1968), and the results of these computations are shown in Appendix B.

2. The Propagation Paths

The VOR station at Gardner, Massachusetts (about 80 km west of Boston), is shown in Fig. 1. This facility is located in hilly, forested terrain on a hilltop cleared of trees. The VHF antenna shown in this figure consists of a conducting ground-plane 150 ft in diameter mounted 15 ft above the ground. A ring of loop antennas 44 ft in diameter is installed one-half wavelength above the ground plane. The pattern of this antenna system is symmetrical in azimuth. The station is a so-called Doppler VOR, described by Anderson and Flint (1959).

We selected propagation paths along azimuth bearings 155, 163, 170, 175, and 190 deg from the transmitter. These paths are shown plotted on a contour map in Fig. 2. Propagation was measured over six paths extending from the VOR to points labeled in this figure. Nearly all of the terrain along these paths is forested with mixed evergreen and deciduous trees; Fig. 2 shows the areas of forest. We used the 7.5-minute quadrangle maps (scale 1:24,000, contour interval 3.05 m)

CP127-608

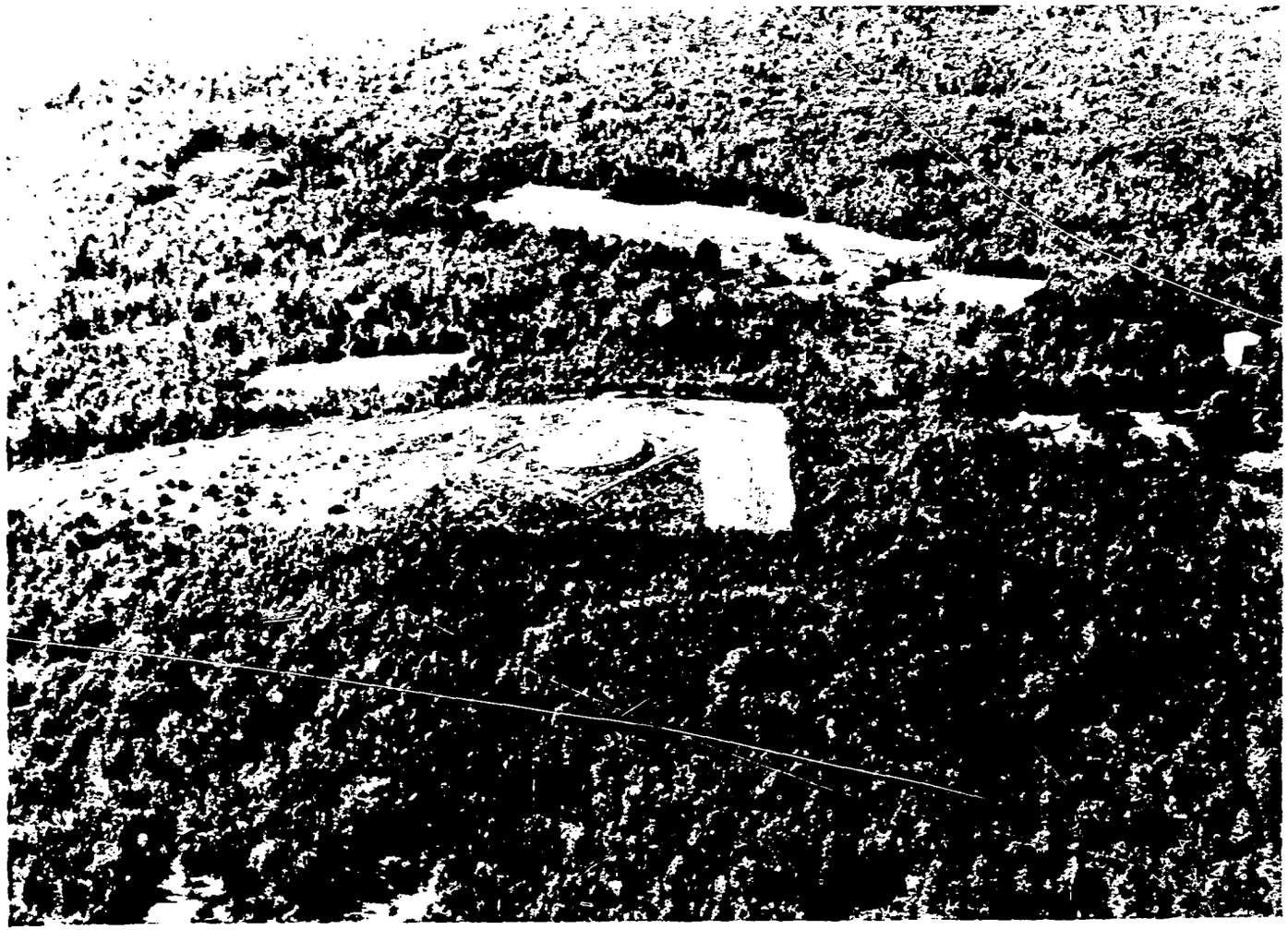

Fig. 1. The VOR Station at Gardner, Massachusetts.

C48-671

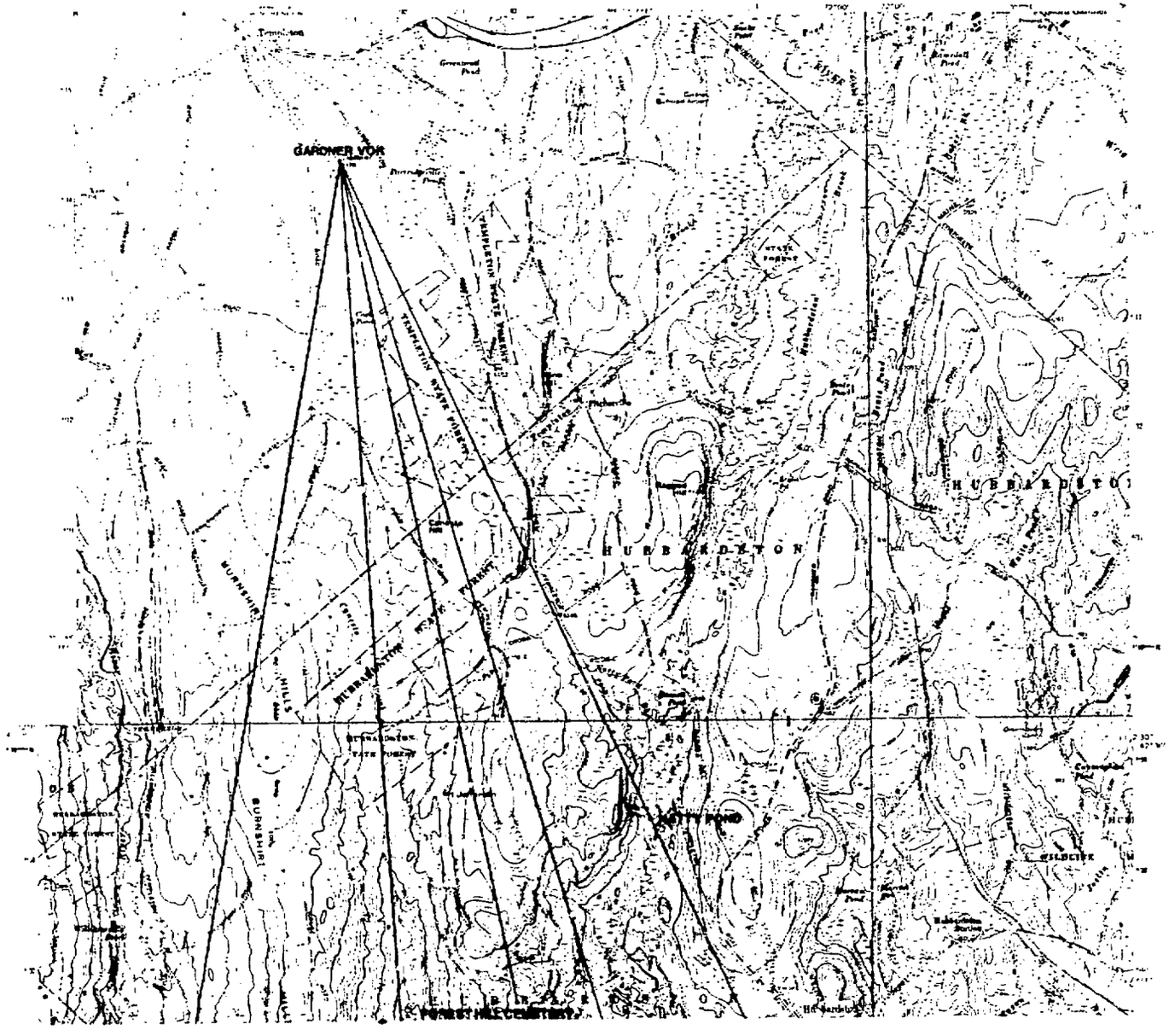

Fig. 2. The Propagation Paths Shown on a Mosaic of Quadrangle Maps.

that are reproduced in Fig. 2 to determine the profiles of the terrain beneath these propagation paths. Straight lines were drawn to represent the paths on the maps; distances to intersections with every contour line were measured and recorded along with the contour elevation. The profile points thus determined were read into a computer and interpolated linearly to derive a profile represented by points equally spaced 10 m apart along each path. Figure 3 shows the terrain profiles. Note that several maxima show up on each profile. In Fig. 3 we find a ridge in the Natty Pond-West Ware River profile at a distance of 4 km that will mask the line-of-sight when the helicopter is at low altitudes over the measurement points. In the other profiles at distances from 2.4 to 5.2 km there are also predominant ridges that mask the line-of-site at low altitudes.

We selected these profiles for propagation measurements because they present several difficulties for propagation modeling: (1) several ridges or hills appear in each profile, so that multiple-knife-edge diffraction may occur when the receiver is at low altitudes, (2) significant portions of terrain profiles lie within the first Fresnel zone when the receiver is near but above the predominant mask, and (3) when the receiver is below the predominant mask, large portions of the terrain between transmitter and mask also lie within the first Fresnel zone. In other words, when

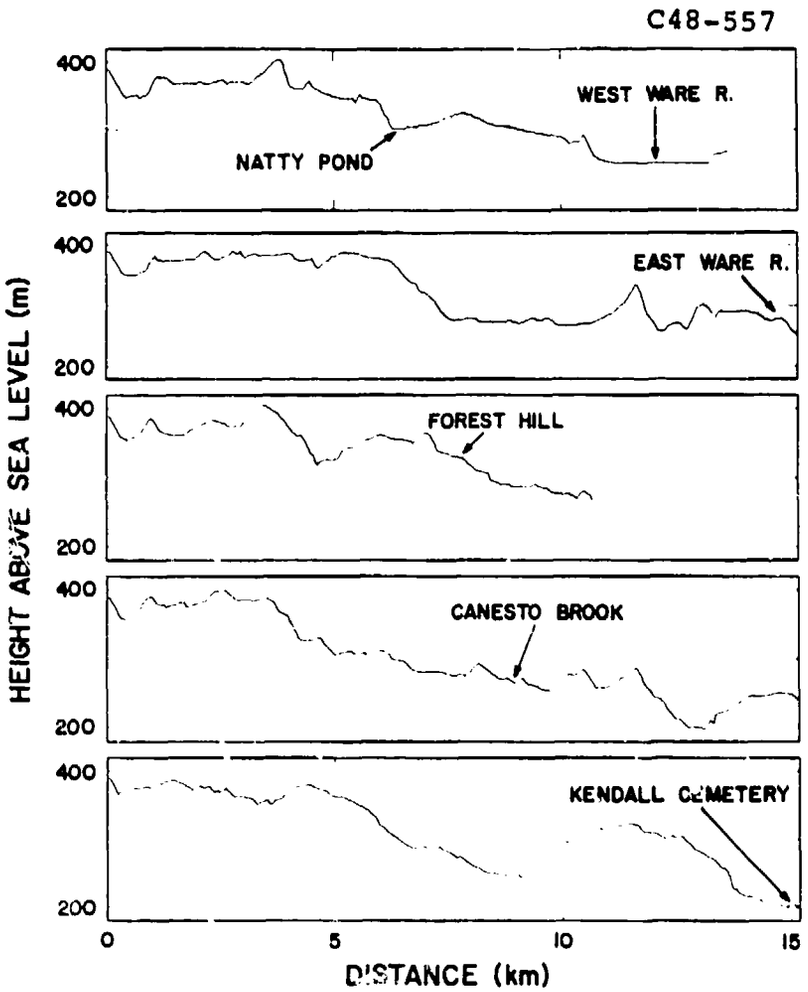

Fig. 3. Terrain Profiles for the Propagation Paths. The locations at which measurements were made are labeled.

the receiver is at low altitudes the first Fresnel zone is obstructed not only by ridges and hills but by large segments of the profiles themselves.

The size of the first Fresnel zone surrounding the geometrical ray paths may be computed from the following expression for H_o, the semiminor axis of the ellipse that forms the outer boundary of the first Fresnel zone: $H_o = (1/2)\sqrt{\lambda R}$, where λ is the wavelength, and R is the distance between transmitter and receiver when there is no masking. If the line-of-sight is interruped by a mask, R is the distance between mask and transmitter (or receiver).

Although we expected little multipath from the forest-covered terrain, we selected two paths, Natty Pond and East Ware River, to test for multipath because these paths have relatively flat terrain in front of the transmitter. If coherent reflection occurred in these areas, it would show up in the vertical-probe measurements over these paths, but no evidence of multipath appears in these data (see Sec. 5). Figure 4 shows an aerial photograph of the terrain along the Natty Pond/West Ware River paths out to a distance of about 5 km from the VOR. This photograph, made at the time of the measurements, shows the evergreen and bare deciduous trees in the forest.

On the basis of earlier measurements of diffraction over trees (LaGrone, 1977 and Meeks, 1981), we assumed that diffraction

Fig. 4. The Area of the Propagation Measurements. An arrow indicates the position of the VOR station; the line shows the first 5 km of the Natty Pond path.

occurred at treetop heights, so it was necessary to take into account the tree cover on the predominant masks. This was done by making theodolite measurements from the VOR site along each path to determine the elevation angles of the mask. Tree heights were then determined by subtracting the elevation angles of the bare hilltops computed from the relief-map data. An average tree height of 50 ft (15.2 m) was determined in this way, and this height was added to the profiles to represent the tree cover in forested parts of the terrain. Before model predictions were computed, the profiles in Fig. 3 were adjusted to include the average tree height. In Appendix A we show additional model predictions for these paths computed with terrain profiles derived from digital terrain-relief data supplied by DMA.

3. Experimental Method

The signal power propagated along each path was measured with a helicopter (Bell 206B) during vertical descents over each path endpoint. In this way the propagated signal was probed as a function of helicopter altitude. Two descents were made over each point. The frequency radiated by the Gardner VOR was 110.6 MHz, the polarization was horizontal, and the transmitting antenna was designed to have isotropic gain in the horizontal plane. Although the gain of the transmitting antenna varies with elevation angle, we have neglected

this effect. All measurements were made at elevation angles between 0 and 5 deg; model measurements of VOR antenna patterns by Sengupta (1971) show that the gain increases by 2 dB when the elevation angle changes from 0 to 5 deg. The receiving antenna on the helicopter was a horizontal dipole mounted below a reflecting plate 80 cm in diameter. When airborne the dipole could be lowered 38 cm below the helicopter landing skids and 57 cm below the reflecting plate. At the beginning of each descent the operator reached through the helicopter window and turned the dipole in a horizontal plane to peak the received signal. Figure 5 shows the antenna on the helicopter with the dipole lowered.

In initial trials the peak received signal was found to be a function of the helicopter heading relative to the line-of-sight. To remove this effect all helicopter descents were made with the helicopter pointed toward the VOR.

The received power was measured with a Singermetrics 37/57 EMI field intensity meter and recorded on a decibel scale with a Hewlett Packard 7155B chart recorder. Figure 6 shows this equipment mounted on the rear seat of the helicopter.

The altitude indicated by the helicopter's barometric altimeter was recorded as a function of time on a cassette audio recorder, and the recording was synchronized with the chart record. In this way we obtained a record of signal strength as a function of receiver height over each path.

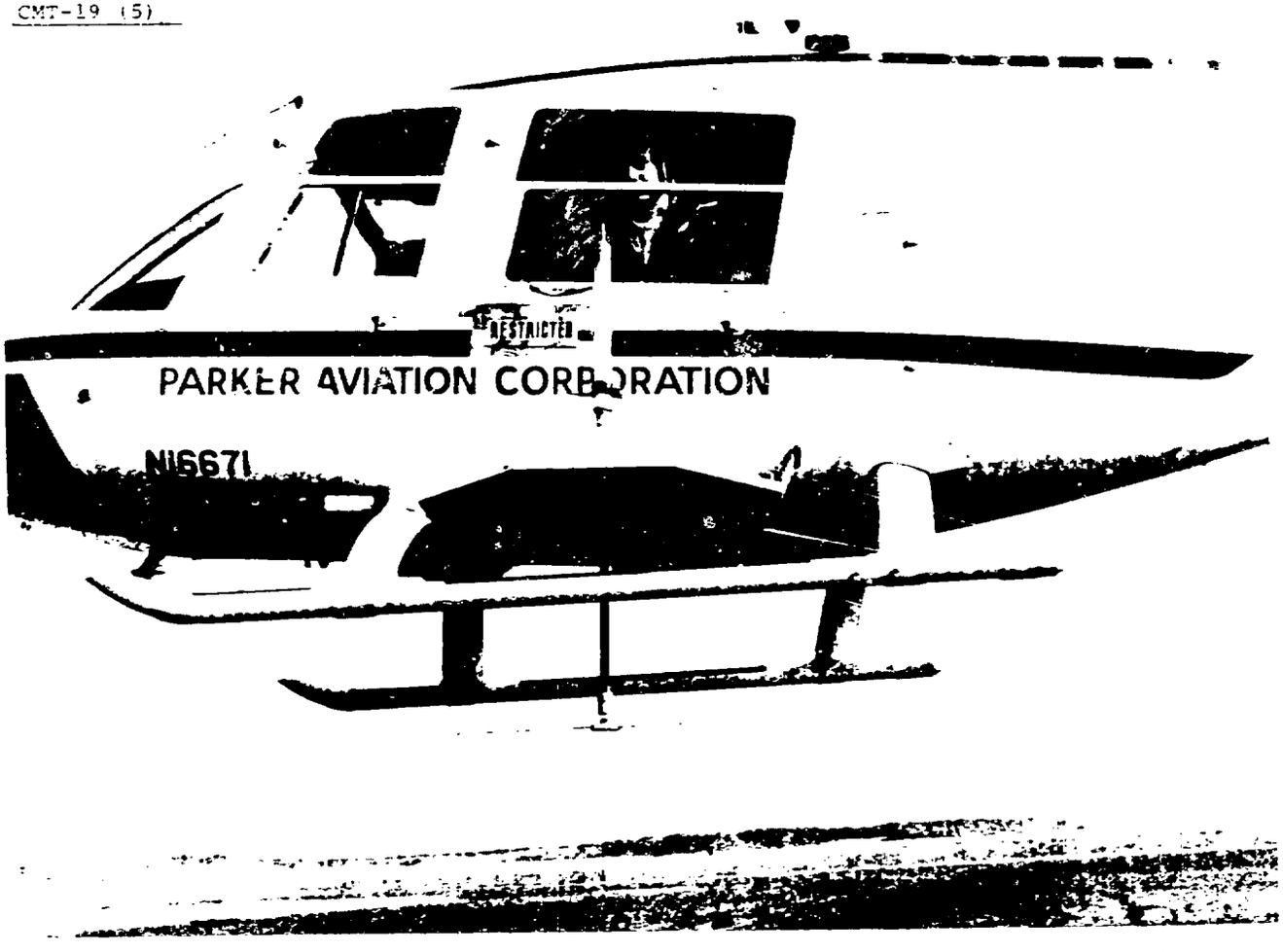

Fig. 5. The VHF Dipole-Antenna Extended Below the Ground Plane.

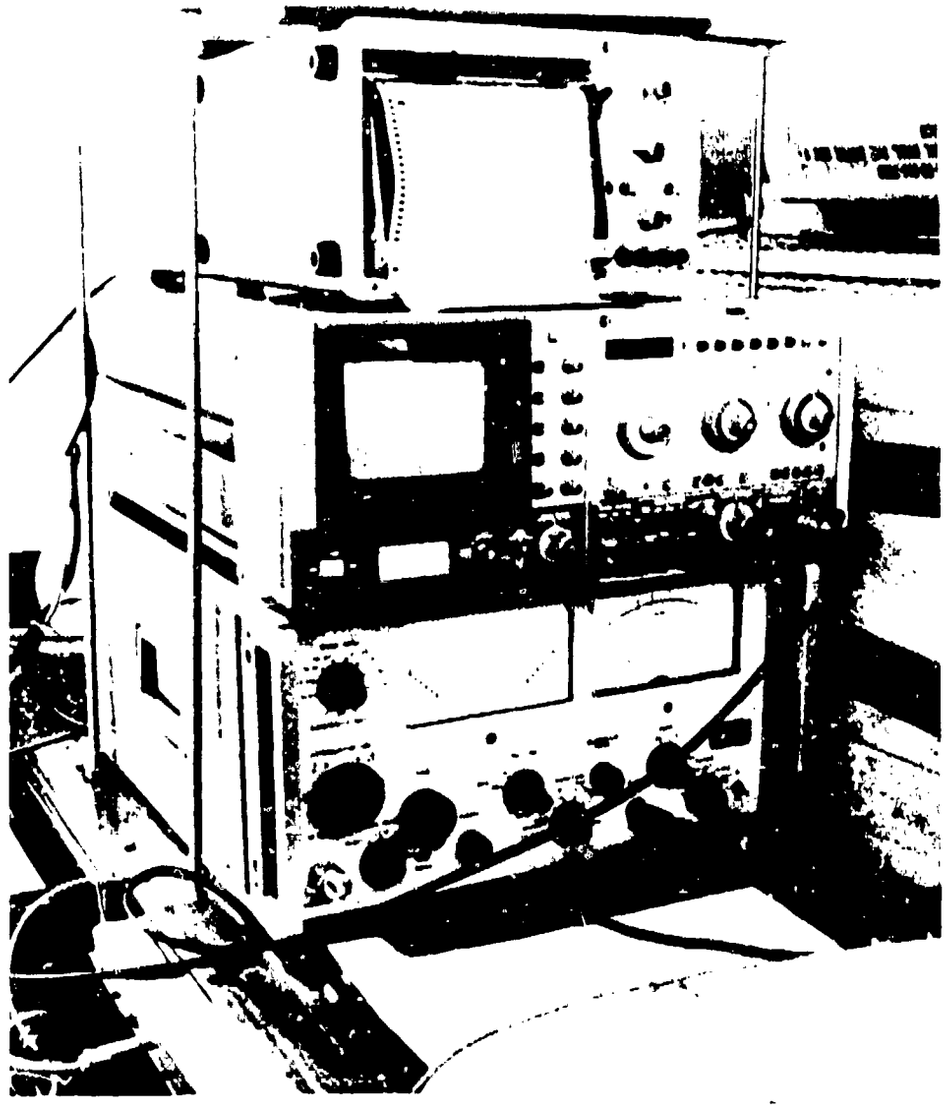

Fig. 6. The Helicopter Instrumentation. The equipment mounted in a rear seat consists of a signal-strength meter, a spectrum analyzer, and a chart recorder.

The descent rates were roughly 3 to 6 m/sec. Taking into account timing errors and altimeter errors, we estimate that the resulting height errors in measuring the signal strength are less than about 5 m.

4. Propagation Modeling

To develop a computer model for predicting VHF propagation over these terrain profiles, we began by considering the modeling as a multiple-diffraction problem, taking the significant diffracting features on the terrain profiles as knife-edges. Several questions then had to be considered: (1) how many knife-edges must be taken into account? (2) how does the computer select these knife-edges? and (3) how is the propagation affected by the fact that much of each terrain profile falls within the first Fresnel zone at the low receiver altitudes? Where the answers to these questions could not be deduced from electromagnetic theory, we tested various assumptions against our measured data to arrive at the computer model described here.

The diffraction produced by a single knife-edge is determined by the position of the diffracting mask in the Fresnel-zone pattern of the propagated wave. The strength of the propagated signal depends on the clearance of the line-of-sight over the knife-edge. As the helicopter descended and the line-of-sight approached the mask from above, diffraction effects began to

become significant when the knife-edge entered the first Fresnel zone. (A detailed discussion of knife-edge diffraction has been given by Meeks, 1981.) Although the problem of diffraction over two successive knife-edges has been solved in terms of Fresnel theory (Millington, et al., 1962), no general solution is available for three or more successive knife-edges. We used an approximate method developed by Deygout (1966) for determining the propagation loss over multiple knife-edges. Figure 7a shows an example of the standard Deygout construction: the loss due to the principal mask M_1 is calculated from the clearance h_1, and the loss due to M_2 from the clearance h_2, constructed as shown. The losses in decibels are added to obtain the total loss. The rationale for this approximation is that knife-edge M_1 may be considered as the origin of a scattered wave that propagates into the shadow region (see Rice, 1954) and is diffracted by M_2, suffering additional loss. This construction can of course be generalized for three or more knife-edges. But we must remember that the scattered edge-wave described by Rice (1954) is only defined at sufficiently large distance from the diffracting knife-edge. Hence this approximation must break down when the separation between knife-edges becomes too small. We can also expect errors when the line-of-sight clears two successive knife-edges, as shown in Fig. 7b. The Deygout approximation takes into

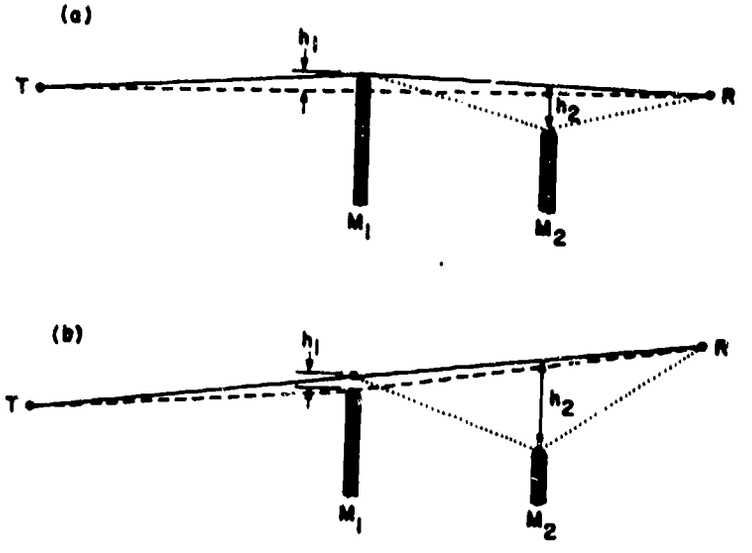

Fig. 7. Ray Constructions for the Extended Deygout Approximation. (a) Shows the standard Deygout construction. (b) Shows the extension by which additional knife- edges are taken into account when there is no masking.

account only one of the cleared knife-edges. We have generalized this approximation as shown in Fig. 7(b). When the line-of-sight clears two masks, the principal-mask contribution is determined as usual from h_1, but the construction shown in Fig. 7(b) is used to determine h_2 so that the effect of the second mask can be taken into account. This change in the construction method insures that the calculated loss will be continuous through the transition between the geometry of Fig. 7(a) and Fig. 7(b).

The computer program that automatically locates the knife-edges on a terrain profile operates as follows. The profile is tested to locate the point of minimum clearance or highest mask between transmitter and receiver, and the location of this point is recorded. If the line-of-sight is unmasked, then the profile is searched for the second highest knife-edge, excluding from the search segments of the profile extending a specified distance (a characteristic length) on either side of the highest knife-edge. A characteristic length of 2 km was used for the calculations discussed here. Similarly, an equal segment around the second knife-edge is excluded, and a search is made for the third highest knife-edge. This process can continue until the entire profile has been covered, or it can terminate after a specified number of knife-edges has been found. In case the line-of-sight

is masked, the lines-of-sight between transmitter and highest mask and receiver and highest mask are subjected to a similar analysis, and we again exclude the profile segments a characteristic length on each side of a knife-edge. The propagation loss is then computed for all the knife-edges located in this way by using the extended Deygout approximation illustrated in Fig. 7.

An example of the knife-edges selected by this program is shown in Fig. 8 for the Kendall Cemetery profile. The knife-edge-search algorithm selected six knife-edges, three slightly different for the top and bottom of the helicopter descent. Note that this algorithm selected knife-edges at ranges of 9.5 and 13.5 km. These points are 2 km, a characteristic length, on each side of the hill at 11.5 km range, and neither point corresponds to a peak in the profile. These points are artifacts of the algorithm, and they suggest the consequences of searching for an unlimited number of knife-edges on a profile by this method. However, we can limit the number of knife-edges to be used, and compare the model predictions for various numbers of diffracting edges.

5. Comparison of Measurements and Model Predictions

To calibrate the received signals with respect to free-space propagation it was necessary to determine the value of a constant representing the product of the gains of the

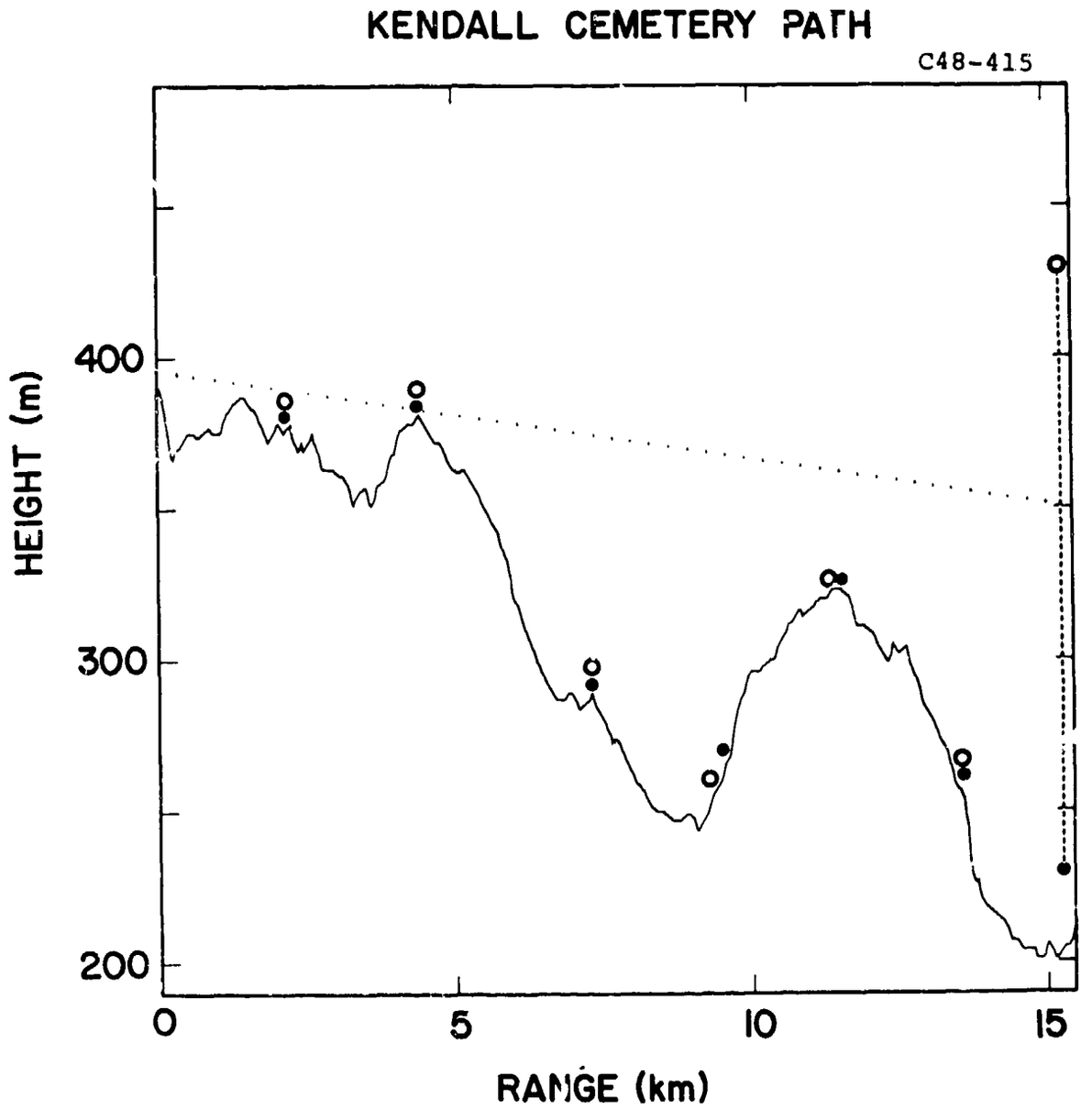

Fig. 8. Knife-Edges Selected by the Computer Program for the Kendall Cemetery Path.

antennas and the radiated power of the transmitter. Choosing the Natty Pond data, we evaluated this constant to obtain a best fit to the model predictions (minimum RMS difference between data and predicted curve). This same correction factor was applied to all other paths. Figures 9 through 14 show the received power measured relative to free-space propagation plotted as points, with the model predictions plotted as lines; the solid lines represent model predictions that include all knife-edges found on the profile and the dashed lines represent the model predictions for a single knife-edge. Circles and dots distinguish the two sets of measurements made over each path. The lowest lines-of-sight over the masks are indicated with the notation LOS. The heights are plotted with respect to sea level, and the prediction curves terminate at ground level. Generally, the two measurements over each path appear to be in excellent agreement. The model predictions for a full set of knife-edges shown by the solid lines match the measurements well. Predictions made using the single most prominent knife-edges (dashed lines) are also in good agreement except near the ground for some of the paths, notably East Ware River and Kendall Cemetery. For these two paths the terrain profiles in Fig. 3 show prominent secondary knife-edges that mask the receiver

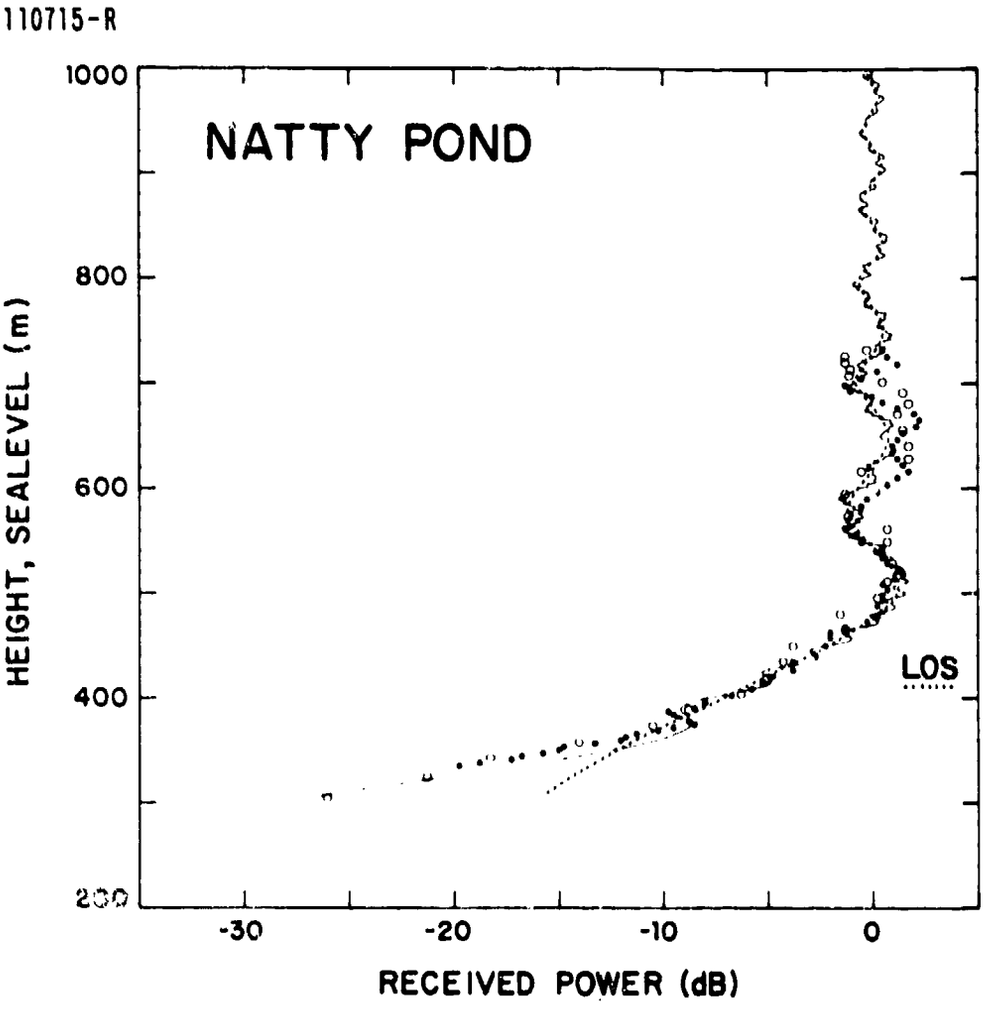

Fig. 9. Vertical Probe for the Natty Pond Path. Data from two sets of measurements are plotted as points; the solid curve represents the prediction of the multiple-diffraction model with no limit on the number of knife-edges. The dotted curve represents the predictions for a single knife-edge.

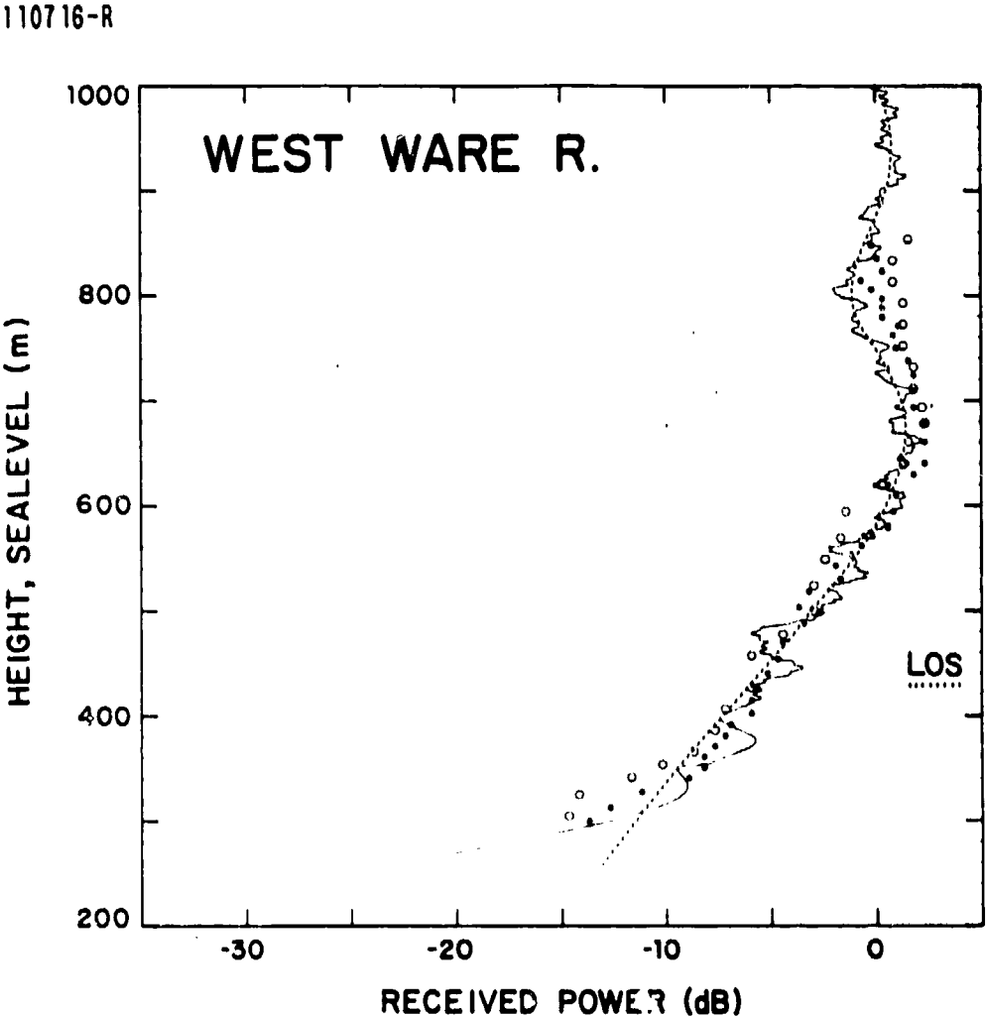

Fig. 10. Vertical Probe for the West Ware River Path. Data from two sets of measurements are plotted as points; the solid curve represents the prediction of the multiple-diffraction model with no limit on the number of knife-edges. The dotted curve represents the predictions for a single knife-edge.

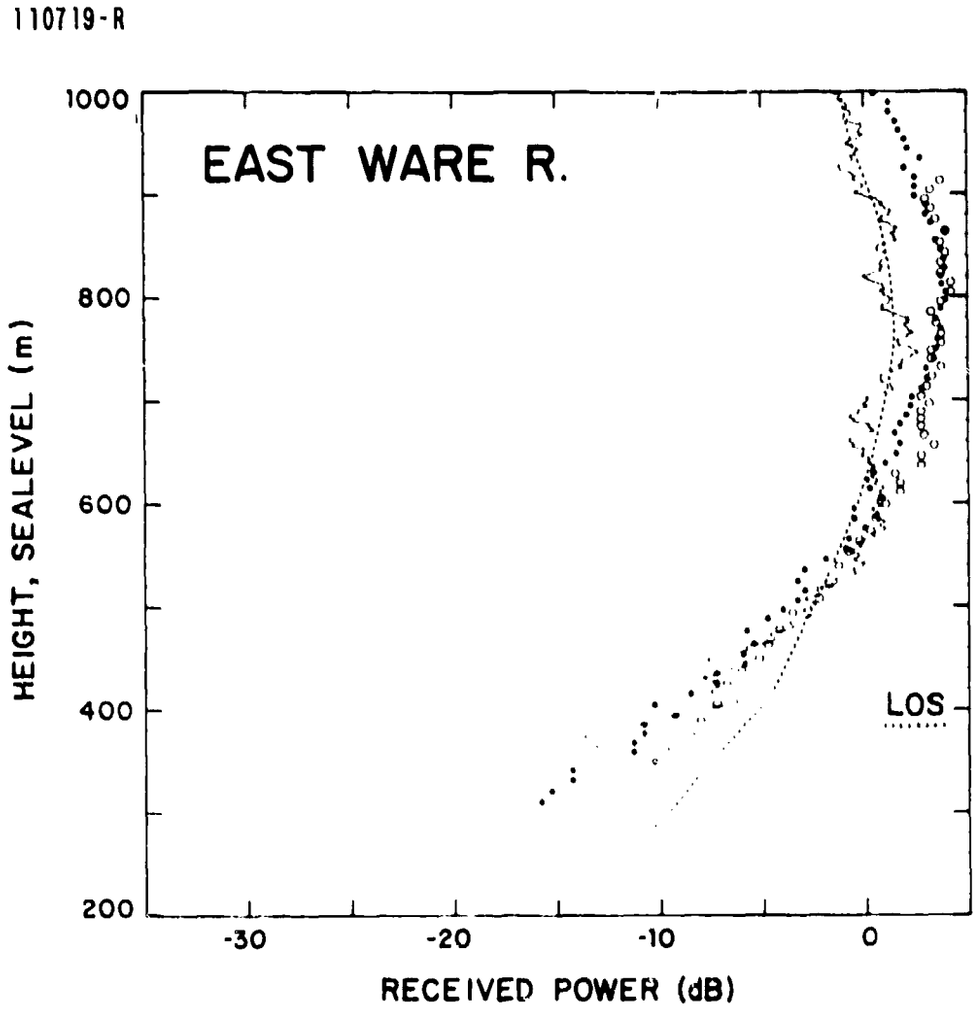

Fig. 11. Vertical Probe for the East Ware River Path. Data from two sets of measurements are plotted as points; the solid curve represents the prediction of the multiple-diffraction model with no limit on the number of knife-edges. The dotted curve represents the predictions for a single knife-edge.

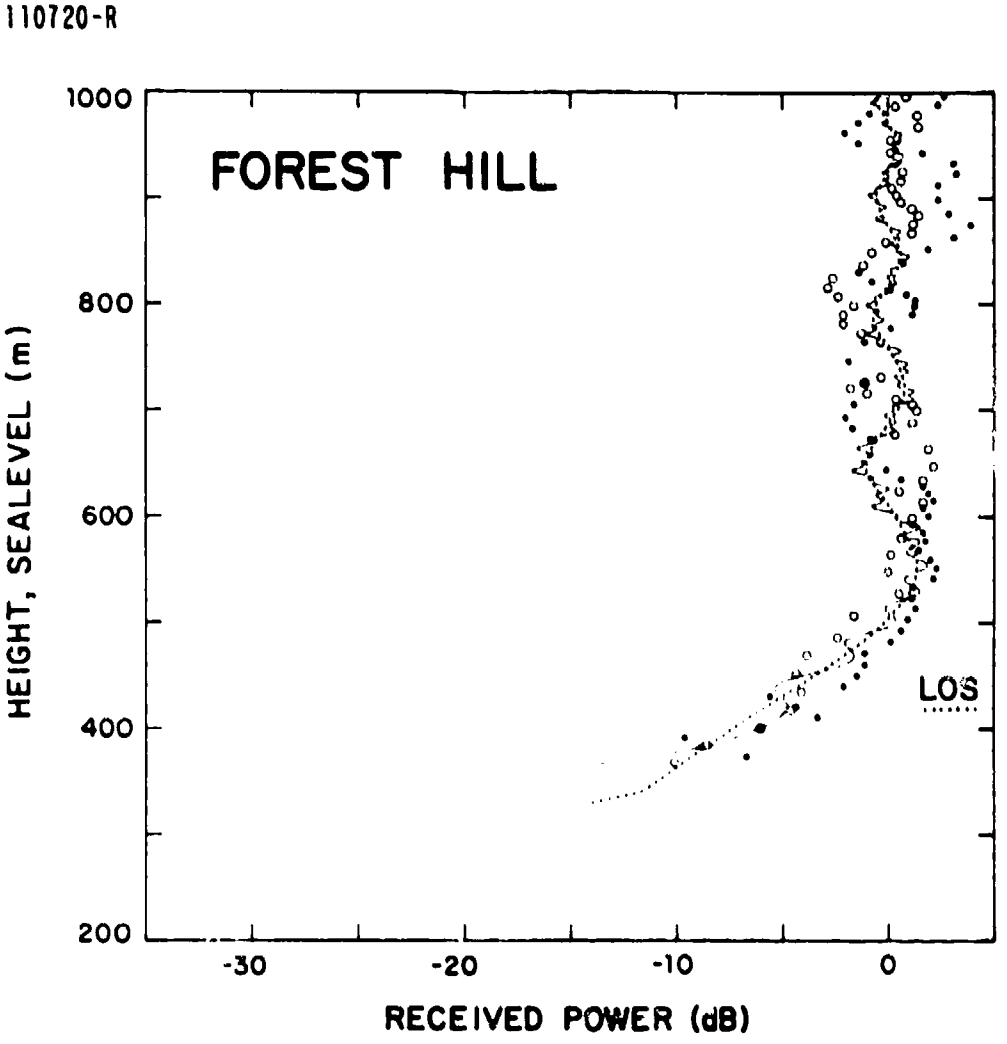

Fig. 12. Vertical Probe for the Forest Hill Path. Data from two sets of measurements are plotted as points; the solid curve represents the prediction of the multiple-diffraction model with no limit on the number of knife-edges. The dotted curve represents the predictions for a single knife-edge.

110718-R

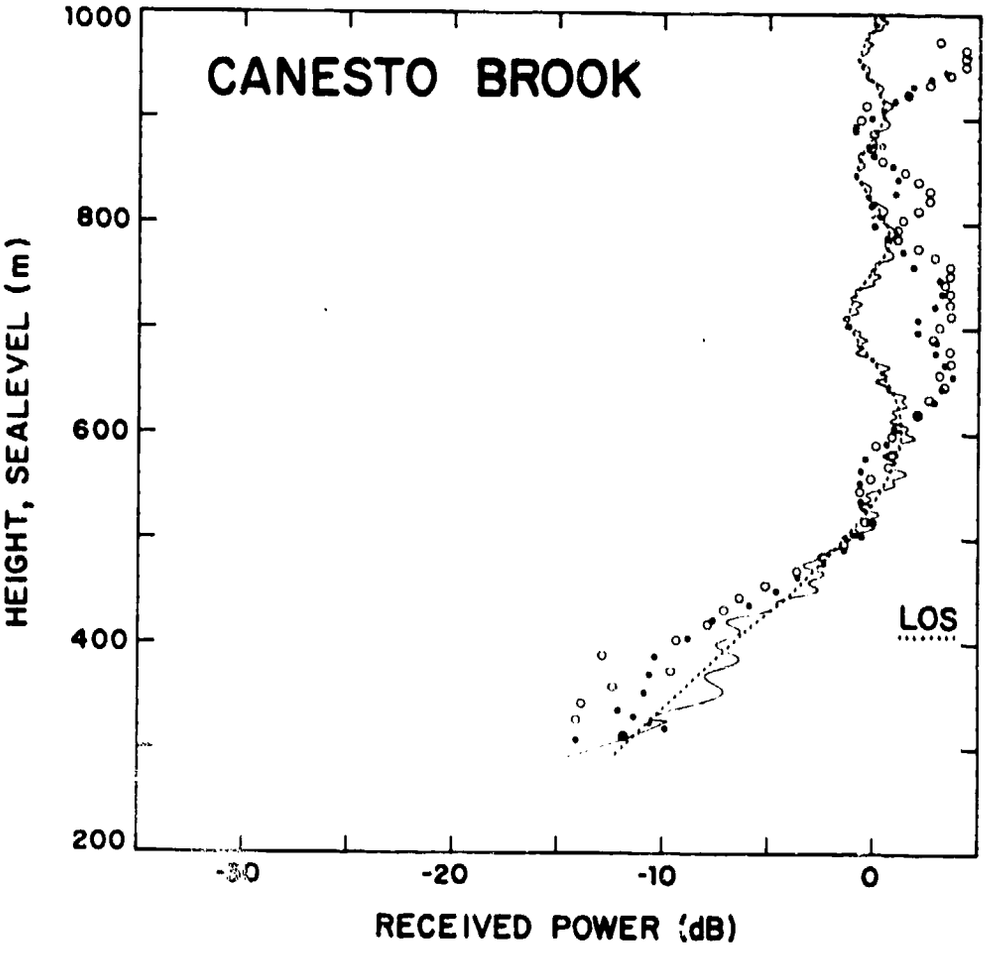

Fig. 13. Vertical Probe for the Canesto Brook Path. Data from two sets of measurements are plotted as points; the solid curve represents the prediction of the multiple-diffraction model with no limit on the number of knife-edges. The dotted curve represents the predictions for a single knife-edge.

110717-R

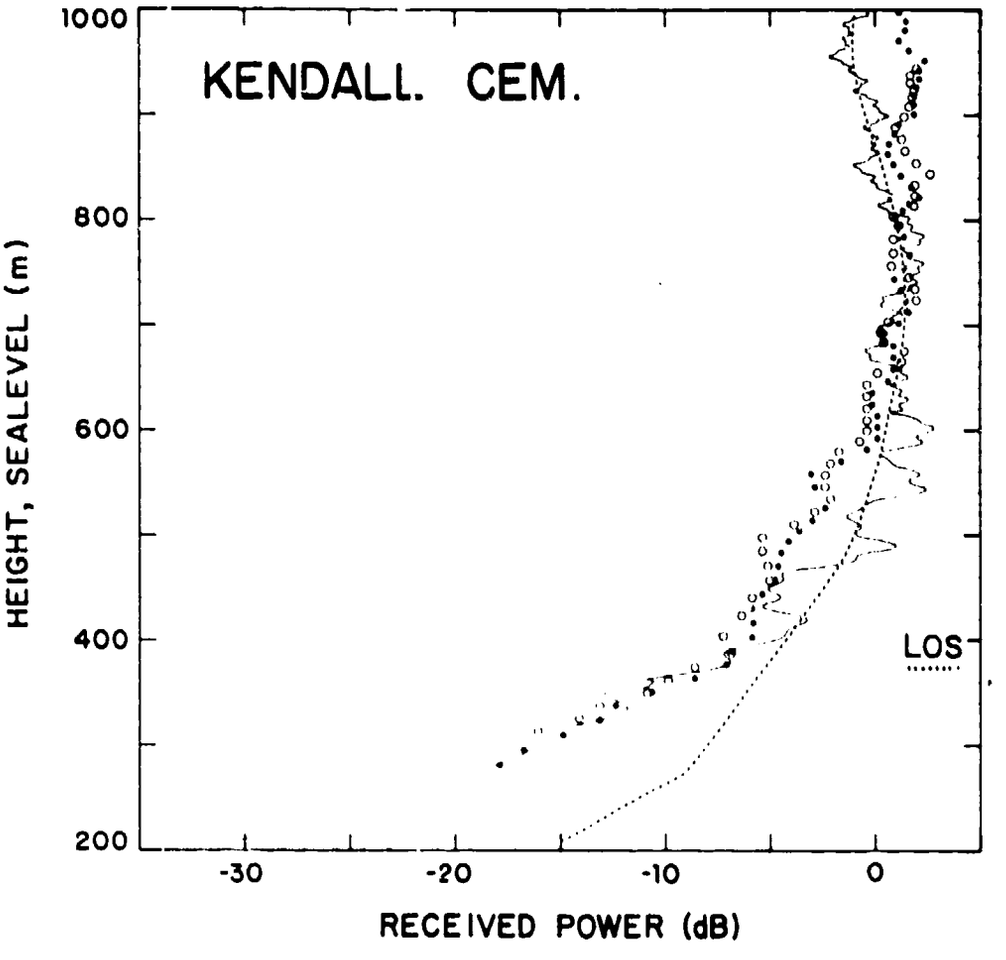

Fig. 14. Vertical Probe for the Kendall Cemetery Path. Data from two sets of measurements are plotted as points; the solid curve represents the prediction of the multiple-diffraction model with no limit on the number of knife-edges. The dotted curve represents the predictions for a single knife-edge.

at low altitudes, and these second knife-edges need to be taken into account. The fine-scale ripples that appear on the solid lines but not on the dashed lines are produced by the additional knife-edges found when the number is not limited.

Table 5.1 summarizes the degree of agreement between the data and the model for various numbers of knife-edges. We have included in this table predictions for single, double, and multiple knife-edges. Note that the predictions for multiple knife-edges are not significantly different from the predictions for double knife-edges. As expected, the single-knife-edge predictions for the East Ware River and Kendall Cemetery paths yield larger RMS differences than predictions that include two or more knife-edges.

No evidence of reflection lobes shows up in the measurements made over the Natty Pond and East Ware River profiles where they would be most likely to occur, so the reflection coefficient for this forested terrain must be small at this frequency for the grazing angles encountered. Although large segments of the profiles extended into the first Fresnel zone, our propagation model with two knife-edges nevertheless agrees with the measurements with an RMS error of about 2 dB or less, and the predictions for these profiles are not significantly improved by taking into account more than two knife-edges.

TABLE 5.1

The Propagation Paths and the Deviations Between Measurements and the Predicted Curves for the Single- and Multiple-Knife-Edge Models

Path Name	Distance (km)	Multiple-Knife Edge Model Number of Masks*	Multiple-Knife Edge Model RMS Difference (dB)	Double-Knife-Edge Model RMS Difference (dB)	Single Knife-Edge Model RMS Difference (dB)
Natty Pond	6.6	2, 3	1.25	1.37	1.89
West Ware River	12.5	3, 4	1.37	1.25	1.55
East Ware River	14.8	5, 6	2.48	1.80	2.79
Forest Hill	7.7	2, 3	1.72	1.68	2.00
Canesto Brook	8.1	2, 3	2.44	2.46	2.66
Kendall Cemetery	15.3	6	2.09	1.90	2.85

*Depending on receiver height, the program logic may select different numbers of masks for the same profile.

We have also used the multiple-knife-edge model to predict propagation over these paths with profiles derived from digital terrain-relief maps obtained from DMA. In Appendix A the profiles and the propagation predictions based on DMA data are compared with those derived from Quadrangle Maps. In Appendix B we compare predictions of the Longley-Rice propagation model (Longley & Rice, 1968) with the prediction of our model.

6. Conclusions

VHF radio propagation measured over the paths described here was accurately predicted by a multiple-diffraction model that used a simple generalization of the Deygout approximation. We found it sufficient to represent a terrain profile with two knife-edges even when large segments of the terrain profile were within the first Fresnel zone. The single-knife-edge model predicted the propagation accurately except at low altitudes on some of the paths where a second mask was clearly evident. We found that negligible reflections were produced by this forest-covered terrain.

This multiple-diffraction model should be generally useful for predictions of VHF propagation when multipath reflections from the terrain are negligible. Two knife-edges appear adequate to represent the diffraction effects produced by most terrain profiles. However, the Deygout approximation cannot be used for closely spaced knife-edges, and we cannot easily define the spacing at which the Deygout approximation

breaks down. Thus a more accurate solution to the multiple-diffraction problem would make it possible to improve the accuracy of propagation predictions in some cases.

APPENDIX A

PROFILES AND PROPAGATION PREDICTIONS FROM DMA DIGITAL-MAP DATA

To investigate the usefulness of digital-map data generated by the Defense Mapping Agency (DMA) for the prediction of propagation loss, we used the so-called Level 1 Digital Terrain Elevation Data to determine the terrain profiles for the measured paths. The DMA digital-relief maps give terrain elevations in integral numbers of meters over a 3-arcsec grid (spacing 93 m in the north/south direction). These maps were derived by DMA from contour maps, scale 1:250,000 and contour spacing 50 ft. The DMA accuracy specifications* state that the elevation errors are within ±30 m 90 percent of the time. The quadrangle maps, on the other hand, have a scale of 1:24,000, about ten times larger than the maps from which the DMA terrain elevations were derived.

To produce each terrain profile from the DMA data, a great circle was generated at the appropriate azimuth from the location of the Gardner VOR station (latitude 42° 32' 45" N, longitude 72° 03' 32" W). Profile points were located along this great circle at a spacing of 100 m. For each point, the latitude and longitude was determined; then the corresponding grid square in the DMA file was located,

*Product Specifications for Digital Landmass System (DLMS) Data Base, Defense Mapping Agency, Aerospace Center, St. Louis AFS, MO, Stock No. SPEC X DLMS (July 1977).

and the elevation was determined by a two dimensional interpolation (in latitude and longitude) from the four DMA points defining the grid square. The resulting profile was then sampled with 10-m spacing, the terrain height being determined by linear interpolation between the neighboring points determined with 100-m spacing.

Figures A-1 through A-5 show superimposed plots of profiles derived from each data base and the differences between profile heights (quadrangle data minus DMA data) plotted with the same height scale. Tree heights are not included in the quadrangle profiles. The profiles from DMA data appear smoother, and in almost every case the ridges and hilltops in the quadrangle data are higher than in the DMA data. Dolbier Hill, on which the VOR station is located, does not appear at all in the DMA data. Small height variations in the quadrangle data appear flat in the DMA data. The accuracy limits ±30 m are marked on the plots of profile-elevation difference; one can see that these differences meet the specifications given by DMA for all paths except Forest Hill. The errors exceed ±30 m for the Forest Hill profile over 14 percent of its length in Fig. A-3. However, over the total length of all five profiles these bounds are exceeded only 2 percent of the time.

CMT-19 (A-1)

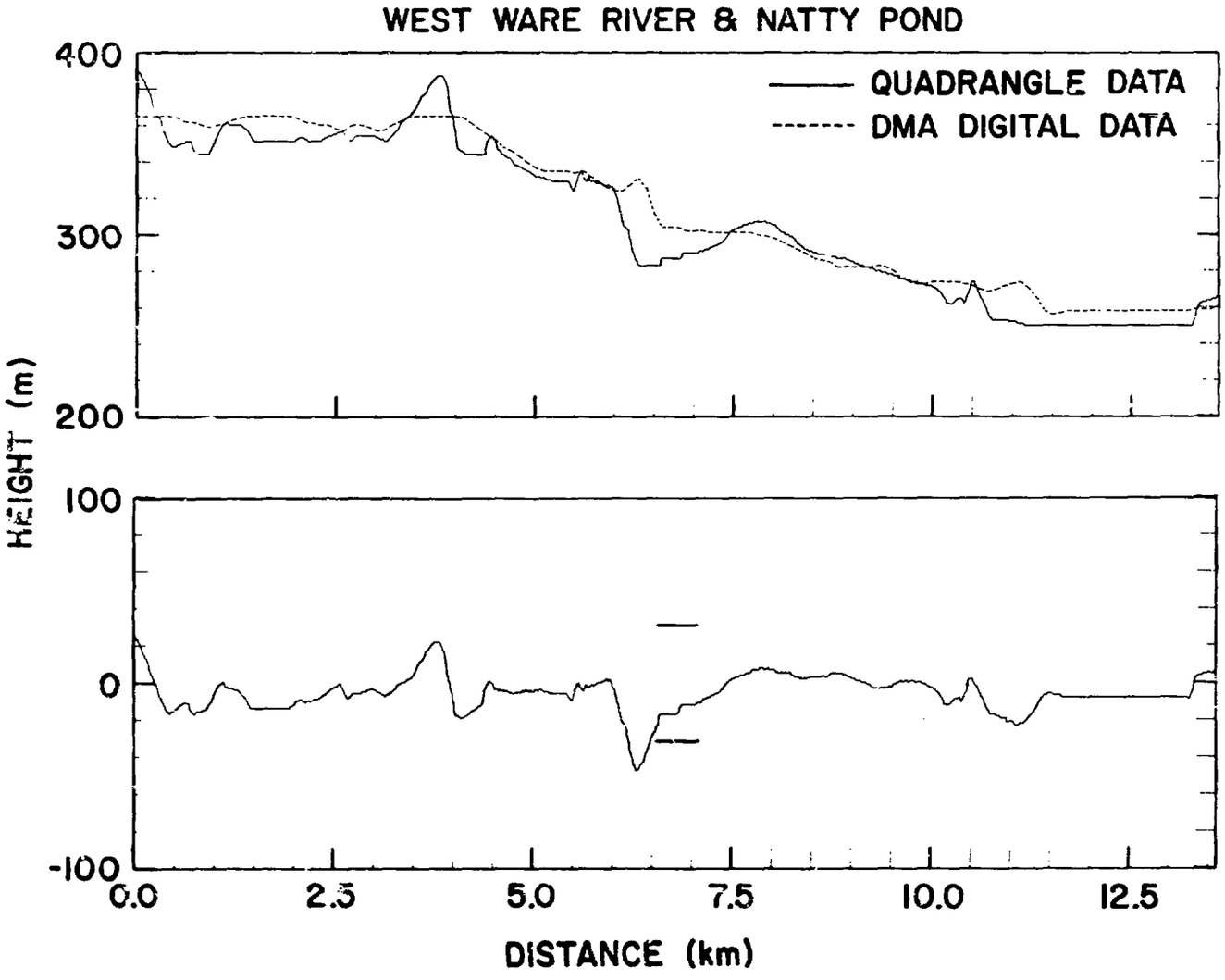

Fig. A-1. Path Profiles and Differences: VOR to West Ware River. The upper curves show profiles derived from quadrangle maps and the DMA digital data; the lower curve shows the difference between these profiles (quadrangle minus DMA) with the ±30 m error limits indicated.

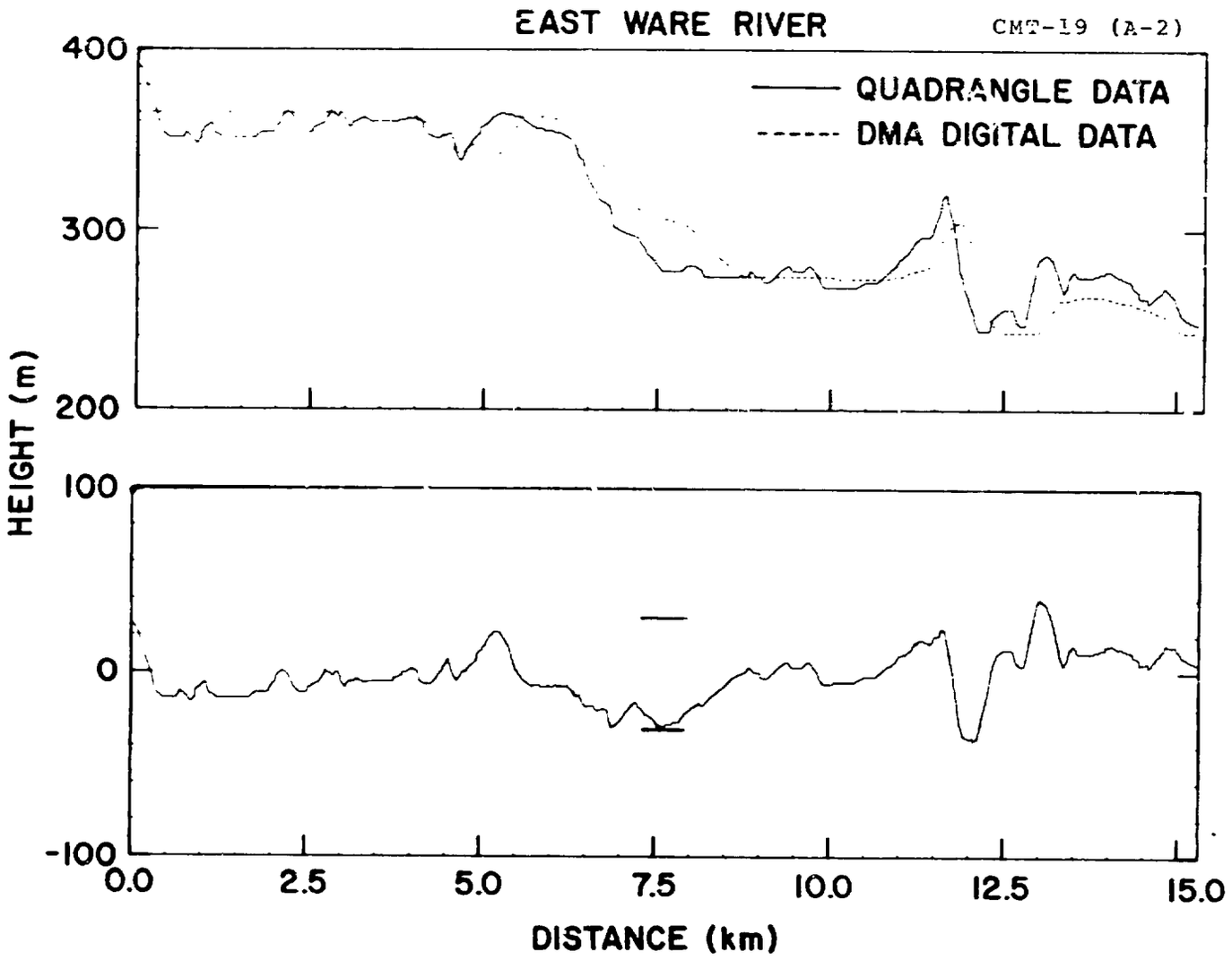

Fig. A-2. Path Profiles and Differences: VOR to East Ware River. The upper curves show profiles derived from quadrangle maps and the DMA digital data; the lower curve shows the difference between these profiles (quadrangle minus DMA) with the ±30 m error limits indicated.

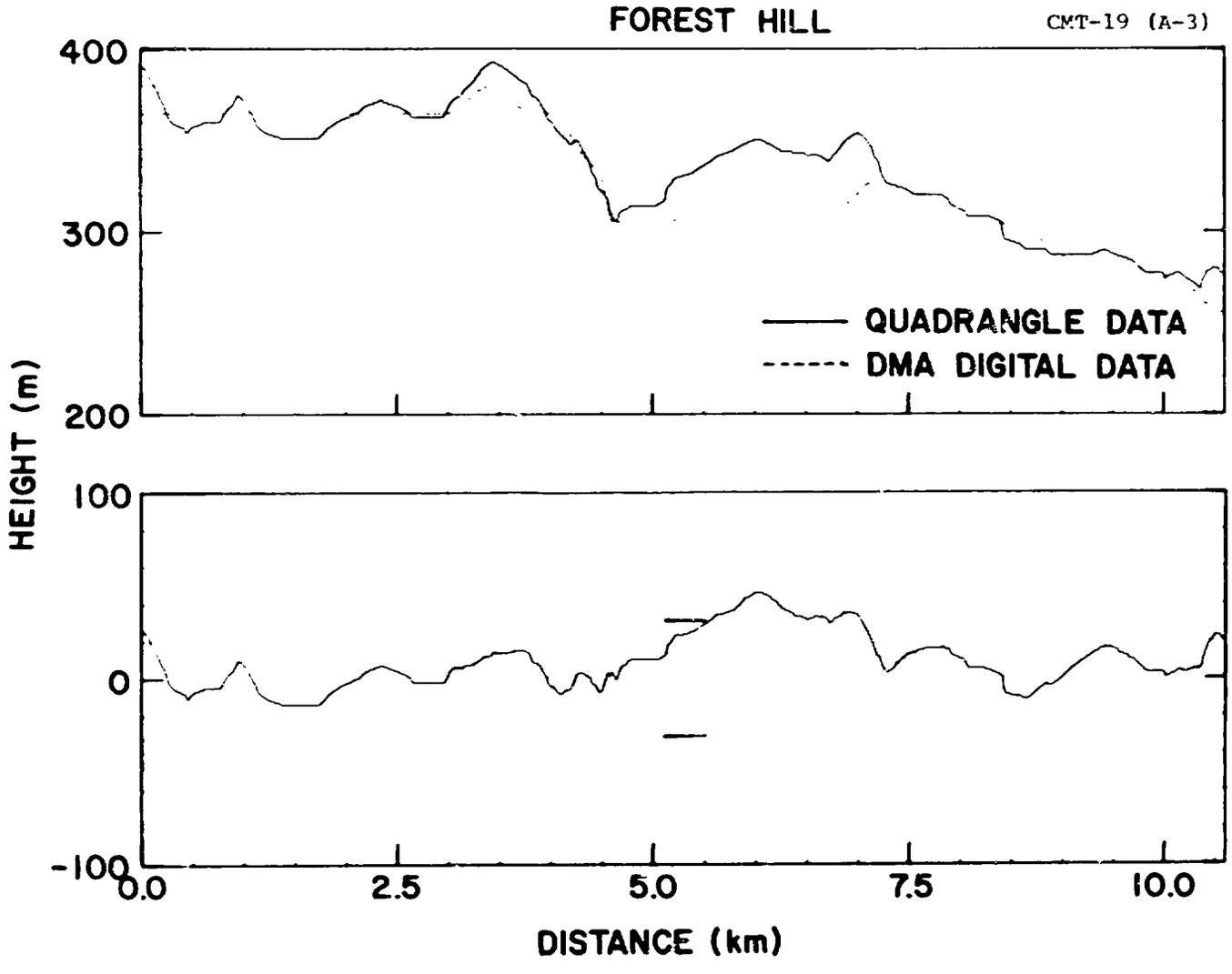

Fig. A-3. Path Profiles and Differences: VOR to Forest Hill. The upper curves show profiles derived from quadrangle maps and the DMA digital data; the lower curve shows the difference between these profiles (quadrangle minus DMA) with the ±30 m error limits indicated.

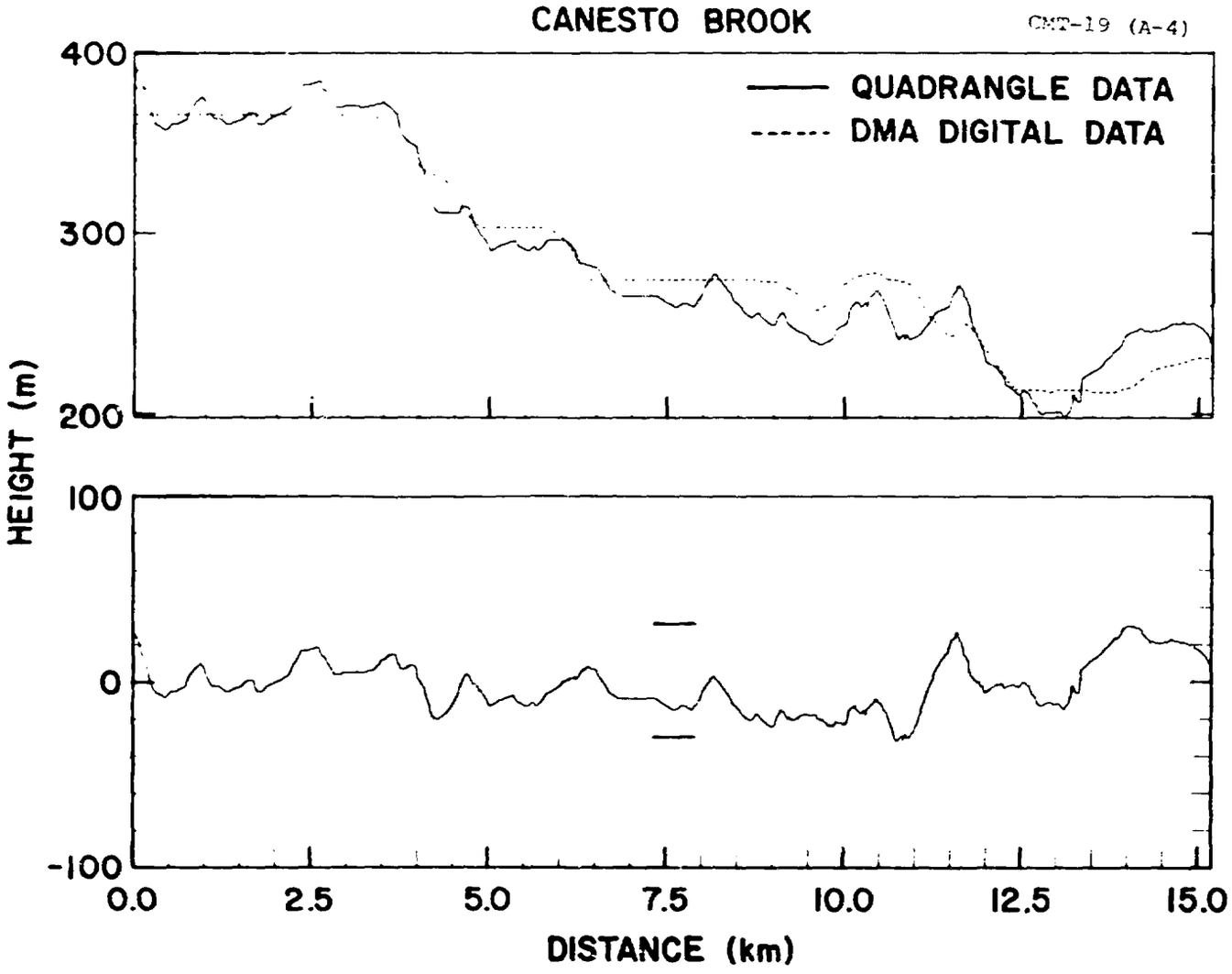

Fig. A-4. Path Profiles and Differences: VOR to Canesto Brook. The upper curves show profiles derived from quadrangle maps and the DMA digital data; the lower curve shows the difference between these profiles (quadrangle minus DMA) with the ±30 m error limits indicated.

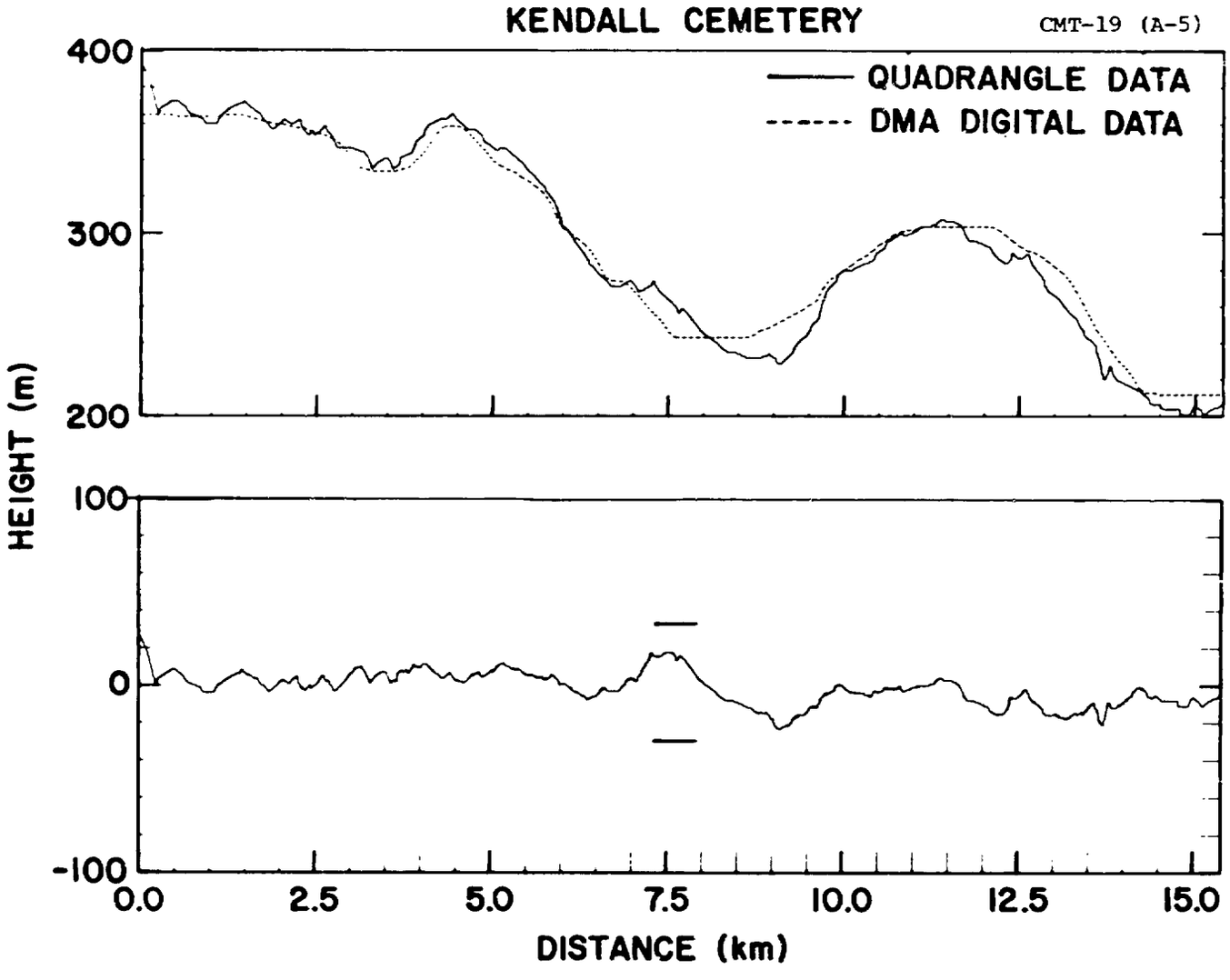

Fig. A-5. Path Profiles and Differences: VOR to Kendall Cemetery. The upper curves show profiles derived from quadrangle maps and the DMA digital data; the lower curve shows the difference between these profiles (quadrangle minus DMA) with the ±30 m error limits indicated.

From the computed differences d_i between elevations on the two profile representations, we have calculated for each of the paths a number of statistical quantities: the mean difference d, the standard deviation σ_d, the RMS difference d_{RMS} ($d_{RMS}^2 = d^2 + \sigma_d^2$), and the correlation length L_c, where L_c is the distance at which the autocorrelation function drops to 1/e. Table A-1 lists these statistical quantities for each path. If we assume that differences have a normal distribution, then we can conclude that 90 percent of the time the differences will lie in the interval $d - 1.65\ \sigma_d$ and $d + 1.65\ \sigma_d$. By this criterion all the paths except Forest Hill easily meet the DMA specification.

The correlation lengths range between 300 and 1140 m in Table A-1. We would expect the correlation length to be related to the smallest detail of terrain relief that can appear on a map of scale 1:250,000. For example, a very small hill might be represented with a circular contour 3 mm in diameter; this would represent a circle of diameter 750 m on the ground, a distance comparable with the range of correlation lengths. The 15-m (50-ft) contour spacing on the maps used to generate the DMA data should be comparable with the values of d_{RMS}, which range between 8.9 and 17.1 m. If the DMA data are to be regarded as a smoothed fit to the

TABLE A-1

ERROR ANALYSIS OF THE DMA PROFILES

Profile Identification	Azimuth (deg)	Range (km)	Mean Error (m)	Standard Deviation (m)	RMS Error (m)	Correlation Length (m)
Natty Pond	155	13.6	-5.9	9.9	11.5	300
East Ware River	163	15.4	-2.0	13.8	13.9	540
Forest Hill	170	10.6	9.0	14.5	17.1	1140
Canesto Brook	175	15.2	-1.9	13.6	13.7	790
Kendall Cemetery	190	15.4	-1.6	8.7	8.9	780

quadrangle data, then the mean differences d in Table A-1 should be small compared to the corresponding σ_d. This appears true for all the paths except Forest Hill and possibly Natty Pond.

Both the quadrangle maps and the DMA digital maps represent ground relief without trees. The treetop elevations were estimated by comparing the theodolite measurements of mask angle with the profiles measured from the quadrangle maps, as described in Sec. 2. We calculated in this way a mean tree height along the masking ridges of 15.2 m with a standard deviation of 2 m. This small standard deviation and the plausible tree height gives us confidence in the quadrangle maps. To investigate the effects of terrain masking, we added the tree height to the quadrangle profiles. If we add 15.2 m to the tree-covered portions of the quadrangle profiles* and calculate the differences between DMA and tree-covered quadrangle profiles, we find from Figs. A-1 through A-5 that the accuracy specifications are met in this case as well; the percentage of profile points with difference outside ±30 m is 7 percent.

We have used the DMA profiles in Figs. A-1 through A-5 to calculate propagation loss with the multiple-knife-

*Dolbier Hill has been cleared of trees.

edge model described in Sec. 4. No limit was set on the number of knife-edges to be used. In Figs. A-6 through A-11 we show the predictions of signal strength (relative to free-space propagation) vs. height plotted as a line; superimposed are the measured data plotted as points, exactly as in Figs. 9 through 14. Table A-2 shows a comparison of the RMS differences in decibels between model predictions and the data for DMA profiles and quadrangle profiles. These figures show that except for the Canesto Brook measurements, the DMA profiles produce good agreement between measurements and predictions. In fact for East Ware River, Forest Hill, and Kendall Cemetery the RMS differences in Table A-1 are smaller for the DMA profiles than for the quadrangle profiles. On those paths for which the quadrangle profiles yield better agreement with measurements, the larger RMS errors from the DMA profiles result because the principal knife-edges are located too low.

110704-R

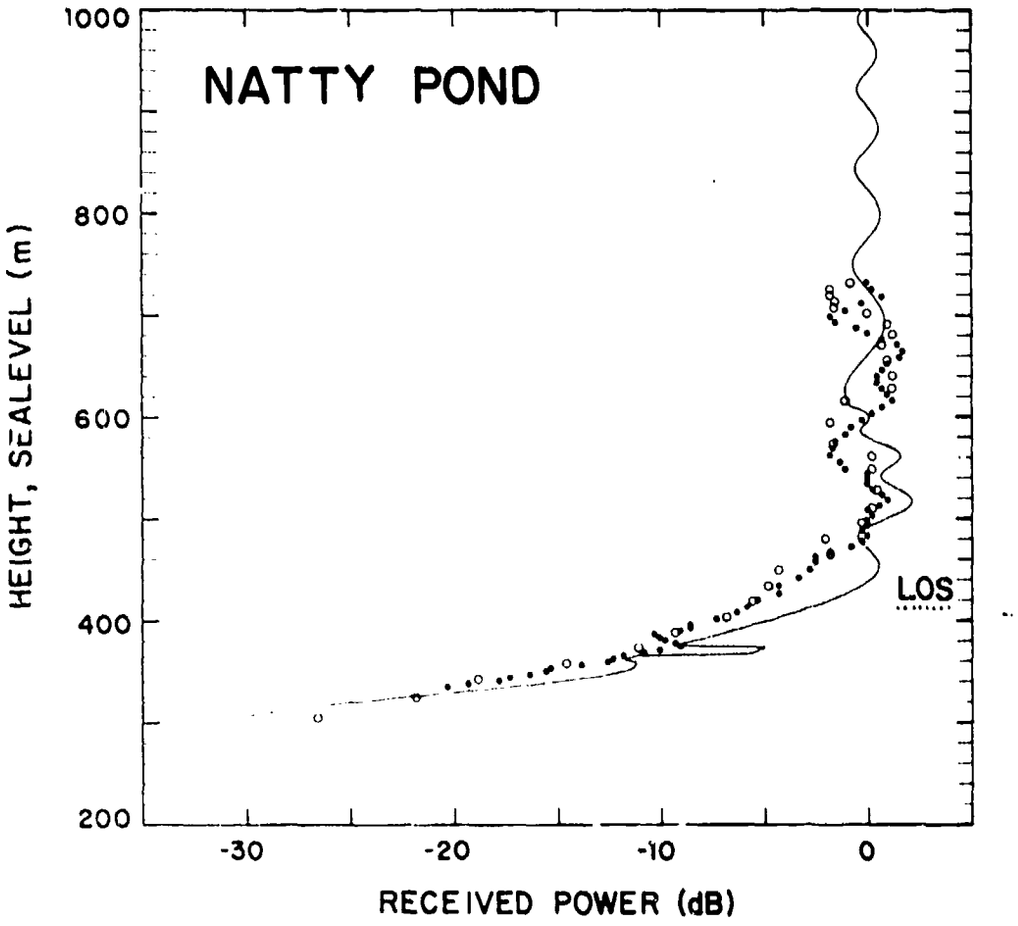

Fig. A-6. Vertical-Probe Measurements and Model Predictions with DMA Data at Natty Pond.

110707-R

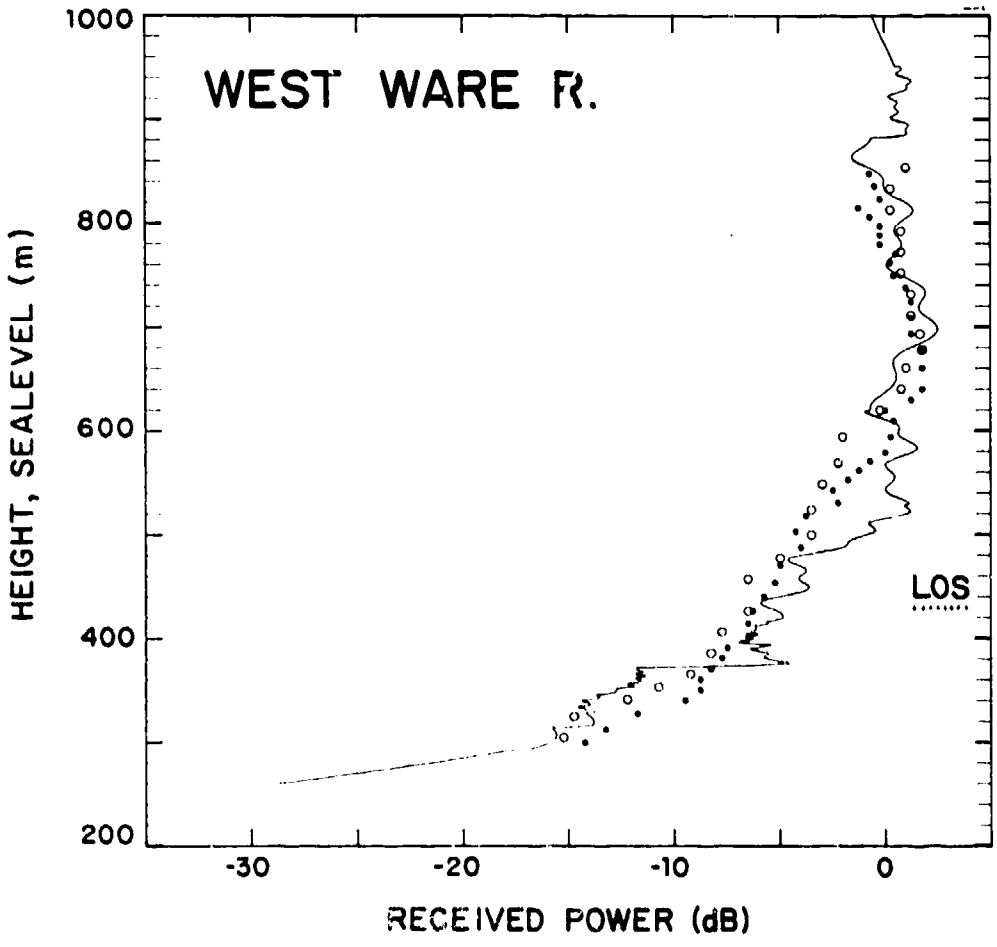

Fig. A-7. Vertical-Probe Measurements and Model Predictions with DMA Data at West Ware River.

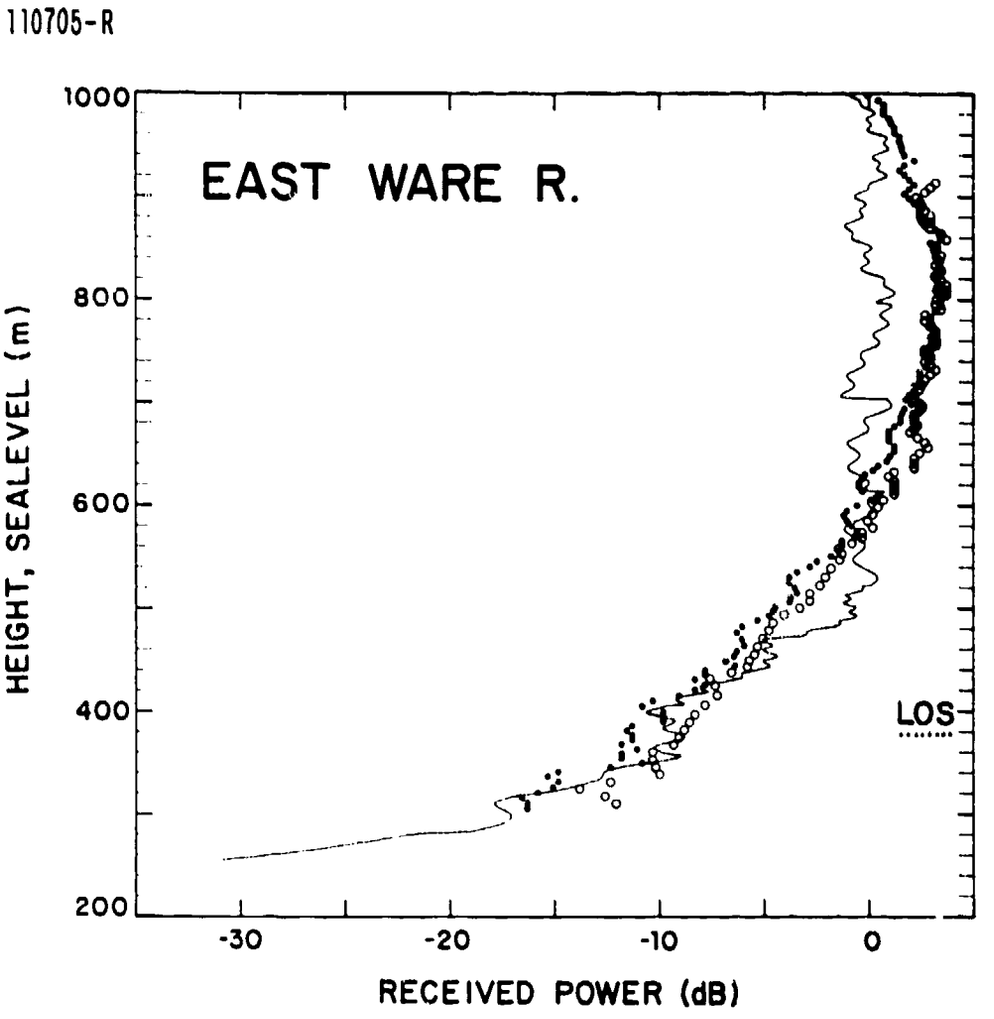

Fig. A-8. Vertical-Probe Measurements and Model Predictions with DMA Data at East Ware River.

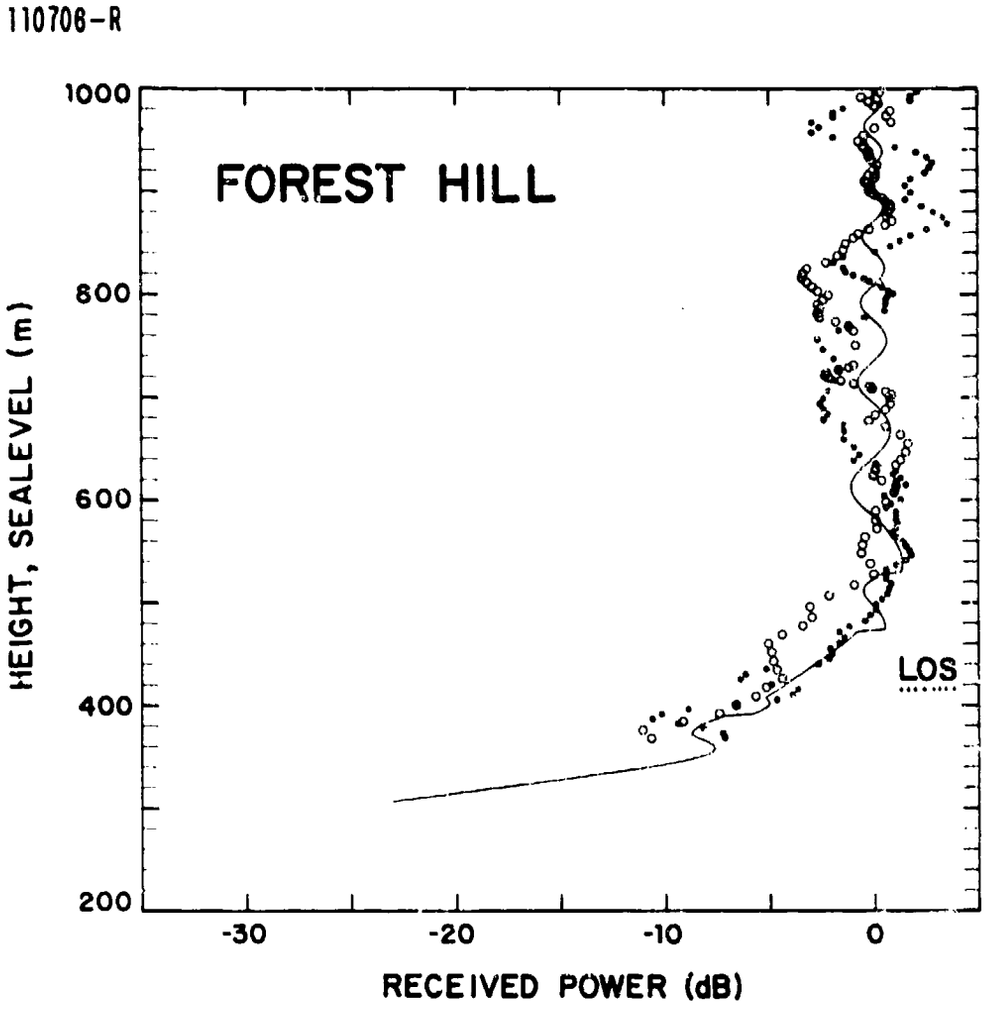

Fig. A-9. Vertical-Probe Measurements and Model Predictions with DMA Data at Forest Hill.

110708-R

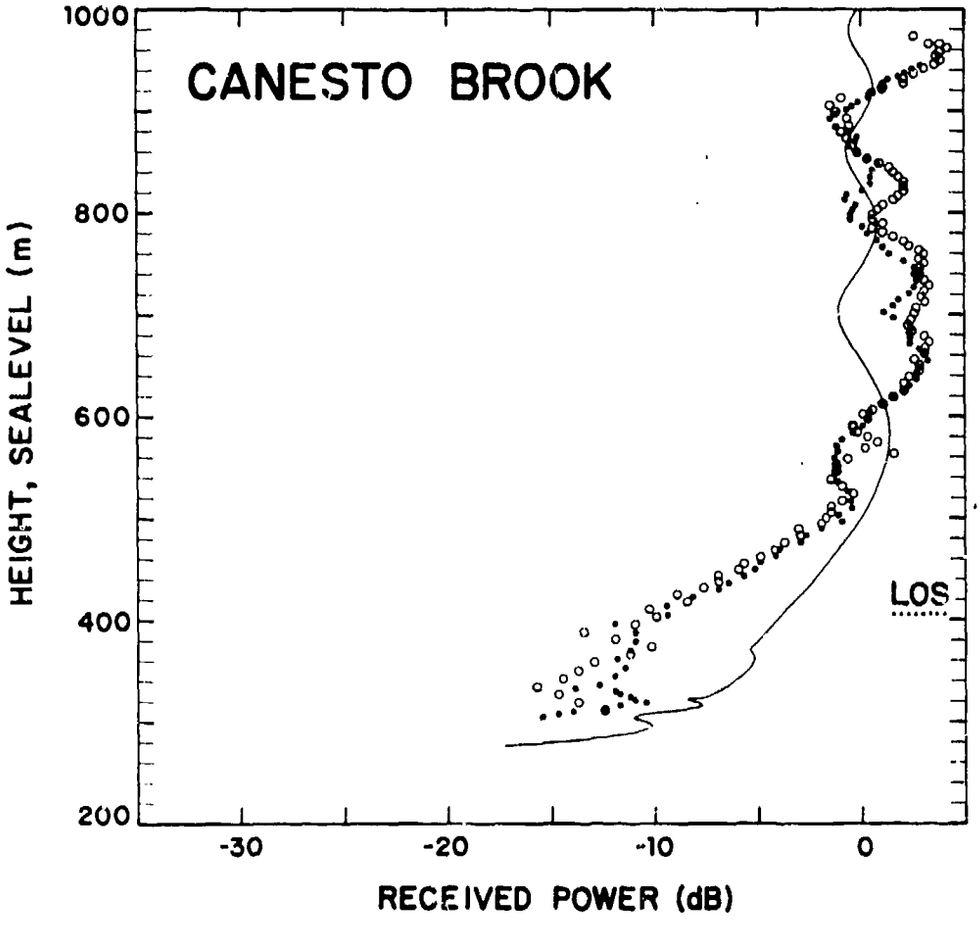

Fig. A-10. Vertical-Probe Measurements and Model Predictions with DMA Data at Canesto Brook.

110721-R

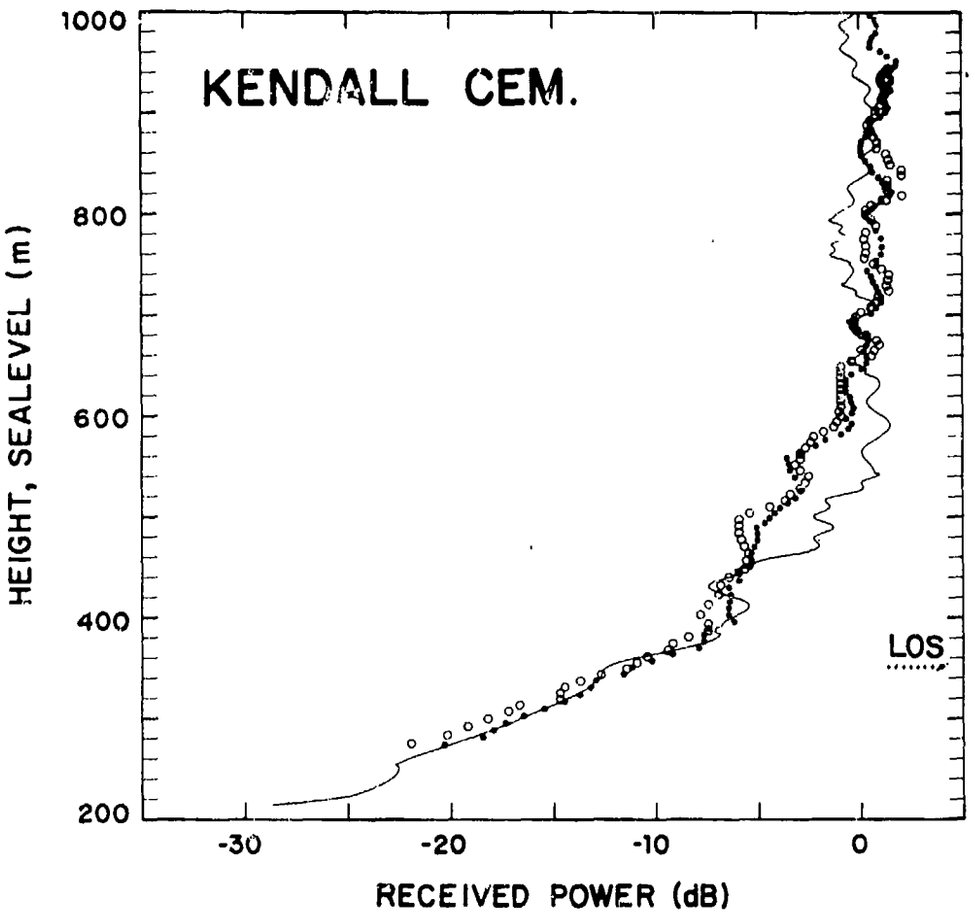

Fig. A-11. Vertical-Probe Measurements and Model Predictions with DMA Data at Kendall Cemetery.

TABLE A-2

COMPARISON OF PROPAGATION-MODEL PREDICTIONS:
DMA PROFILES VS. QUADRANGLE-MAP PROFILES

Path Name	Multiple-Knife-Edge Model RMS Difference (dB)	
	DMA Profile	Quadrangle Map Profile
Natty Pond	2.37	1.25
West Ware River	1.89	1.37
East Ware River	2.30	2.48
Forest Hill	1.65	1.72
Canesto Brook	3.23	2.44
Kendall Cemetery	1.67	2.09

APPENDIX B

COMPARISON OF THE LONGLEY-RICE MODEL AND THE MULTIPLE-DIFFRACTION MODEL

The Longley-Rice propagation model is a widely used computer model for estimating the one-way loss between two ground-based terminals. Because Longley-Rice is a standard model applicable for frequencies from 20 MHz to 20 GHz and for antenna (or target) heights between 0.5 and 3000 m, it is important to compare the predictions of this model with those of our multiple-diffraction model.

The Longley-Rice model computes propagation loss from the following parameters: (1) frequency, (2) polarization, (3) ground conductivity and dielectric constant, (4) atmospheric refractivity at ground level, (5) transmitter and receiver (or target) ground clearances, and (6) the terrain profile between the transmitter and receiver. From the terrain profile the model computes a best-fit straight line to the terrain elevations above sea level and determines the heights of the transmitter and receiver above this line. The heights determined in this way are termed the effective heights. A terrain-roughness parameter is also calculated; it is the so-called interdecile range, the difference between the 90-percentile value and the 10-percentile values of the terrain excursions about this best-fit line. In addition, the model locates the horizon viewed from the transmitter and from the receiver and calculates elevation angles and ranges to these horizons.

Four different types of propagation calculations are contained in the Longley-Rice model; they are the following:

(1) Two-ray interference calculation,

(2) Double-knife-edge diffraction calculation,

(3) Spherical-earth diffraction calculation, and

(4) Tropospheric-scatter calculation.

The tropospheric-scatter calculation influences results only at ranges longer than those considered here. These calculations are approximations to well-known analytical results. For a specific set of input parameters the Longley-Rice model does the following: (1) calculates the loss values at six different ranges using various combinations of the above models, (2) determines a loss at each of these ranges from a weighted average or from an extrapolation of the model calculations, and (3) determines the loss for the specific set of input parameters by interpolation from this set of average losses at the six different path distances.

The Longley-Rice model computation must be regarded as a semi-empirical estimation of the propagation loss, and the accuracy of this model must be judged by comparing its predictions with propagation measurements. Figures B-1 through B-6 show the predictions of the Longley-Rice model superimposed on the measurements. For Forest Hill (Fig. B-4) and Kendall Cemetery (Fig. B-6) the model predictions are in excellent

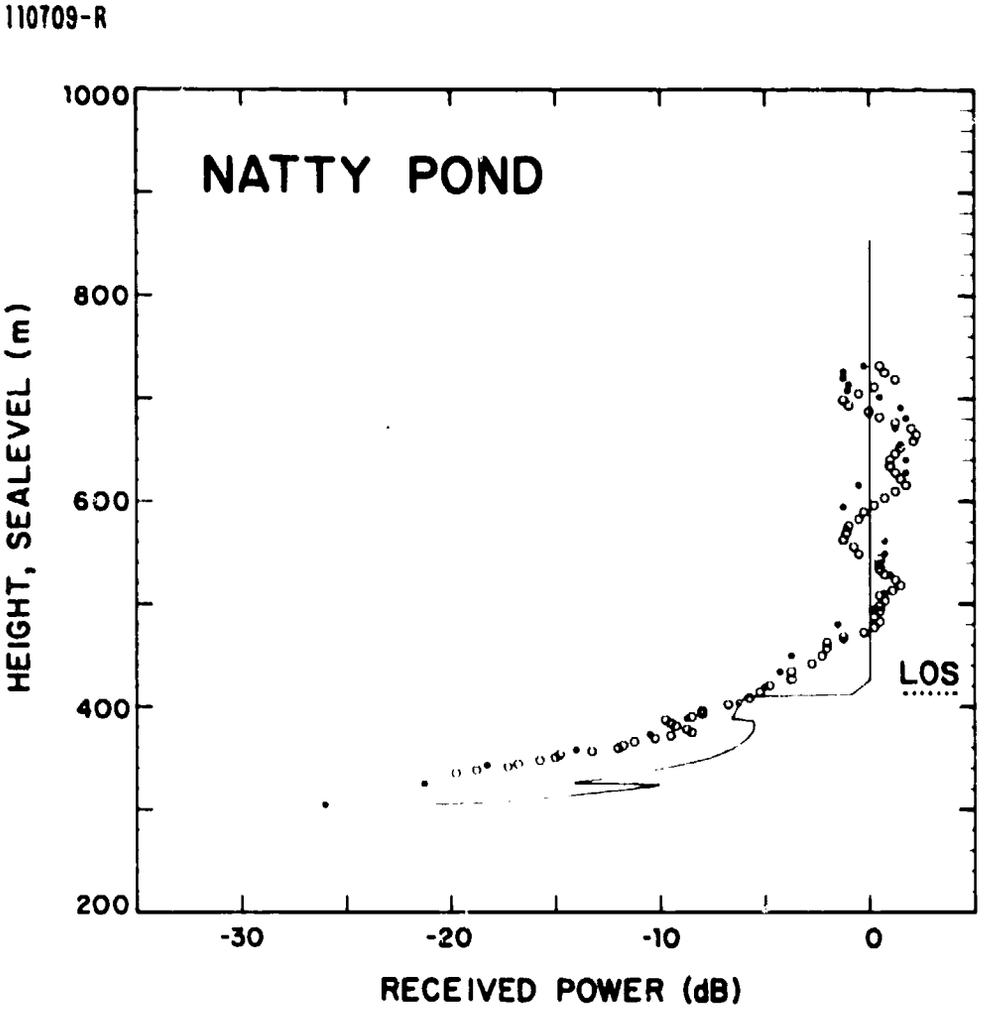

Fig. B-1. Vertical-Probe Measurements and Predictions of the Longley-Rice Model at Natty Pond.

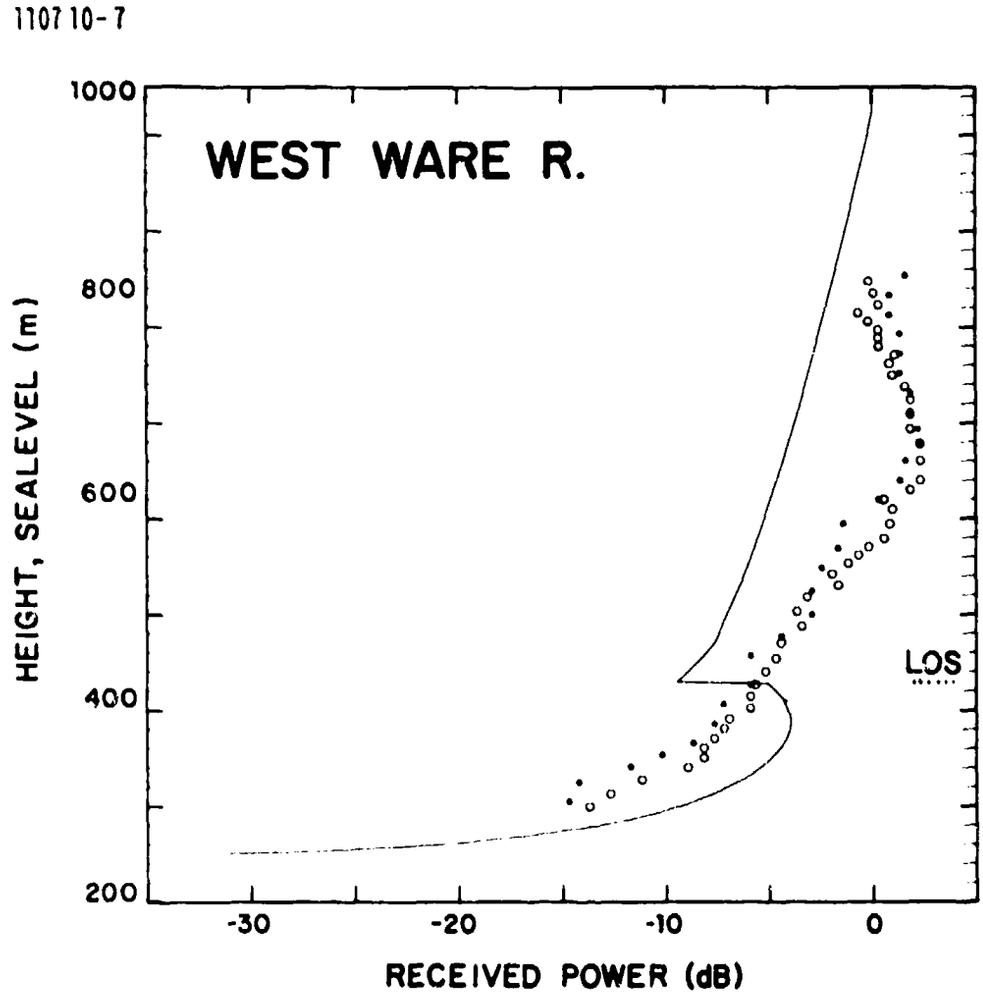

Fig. B-2 · Vertical-Probe Measurements and Predictions of the Longley-Rice Model at West Ware River.

110713-R

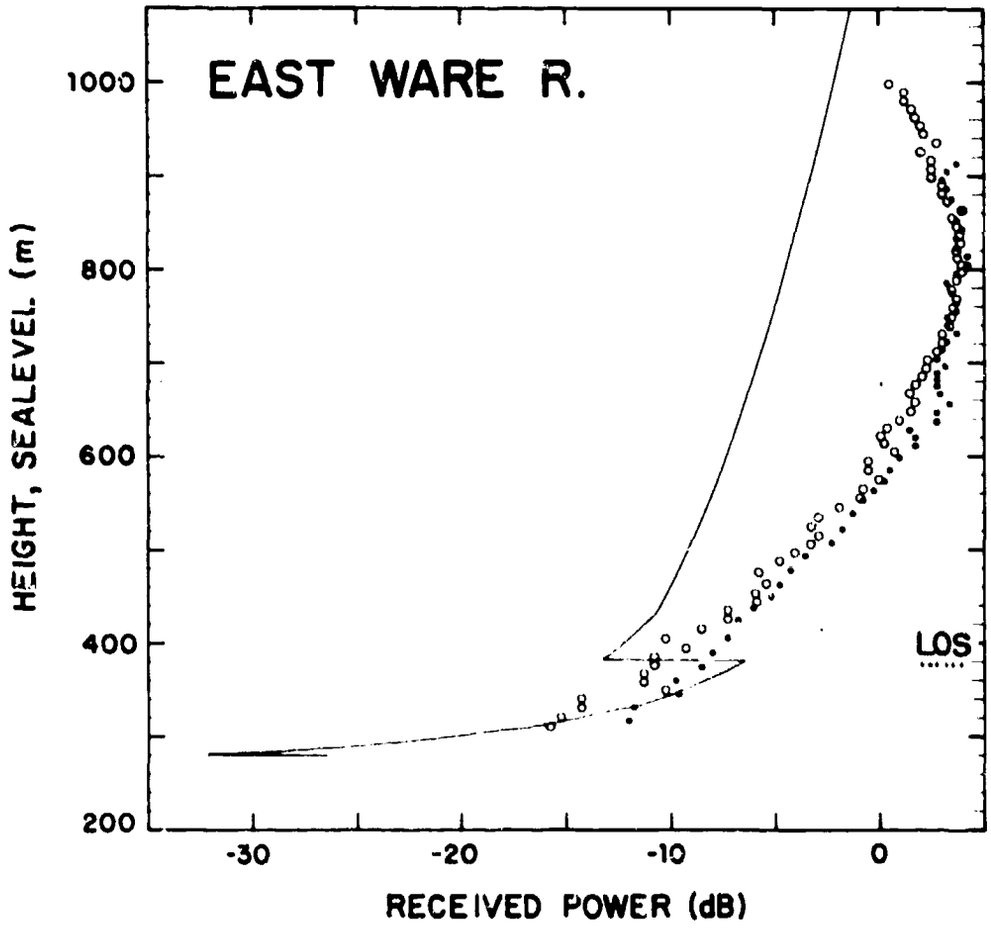

Fig. B-3. Vertical-Probe Measurements and Predictions of the Longley-Rice Model at East Ware River.

110714-R

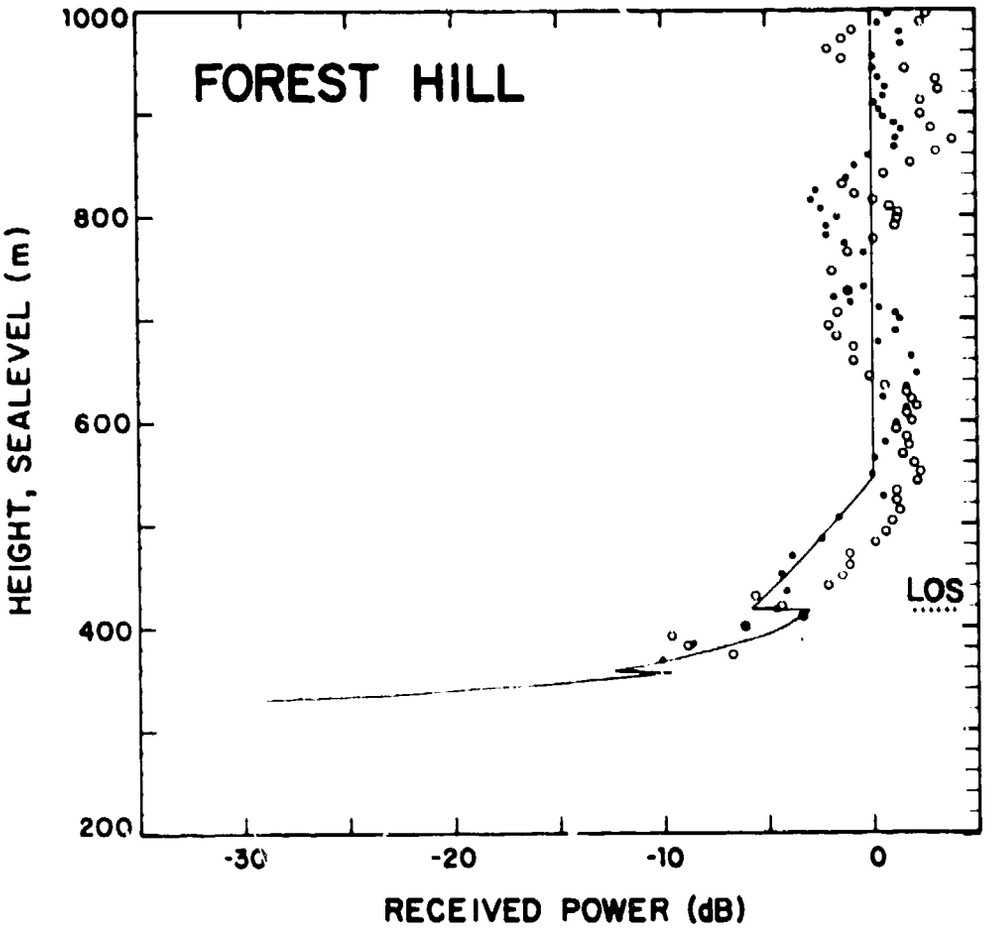

Fig. B-4. Vertical-Probe Measurements and Predictions of the Longley-Rice Model at Forest Hill.

110712-R

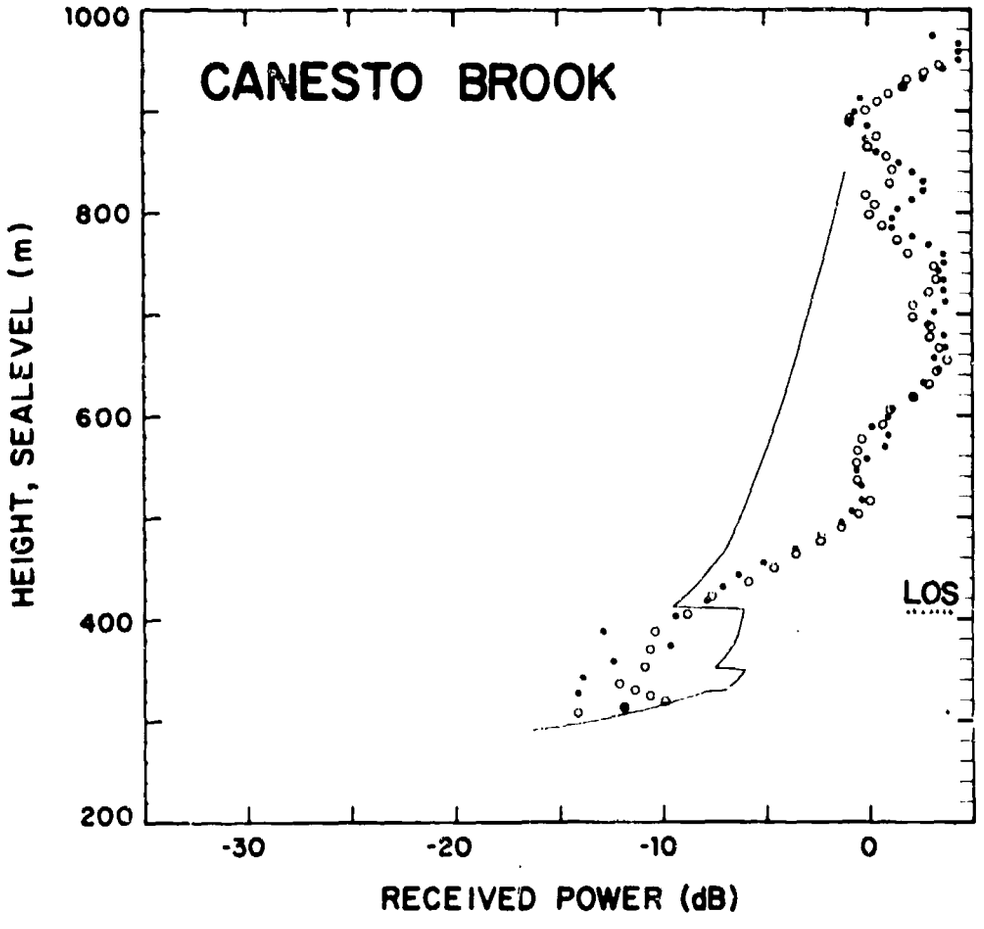

Fig. B-5. Vertical-Probe Measurements and Predictions of the Longley-Rice Model at Canesto Brook.

110711-R

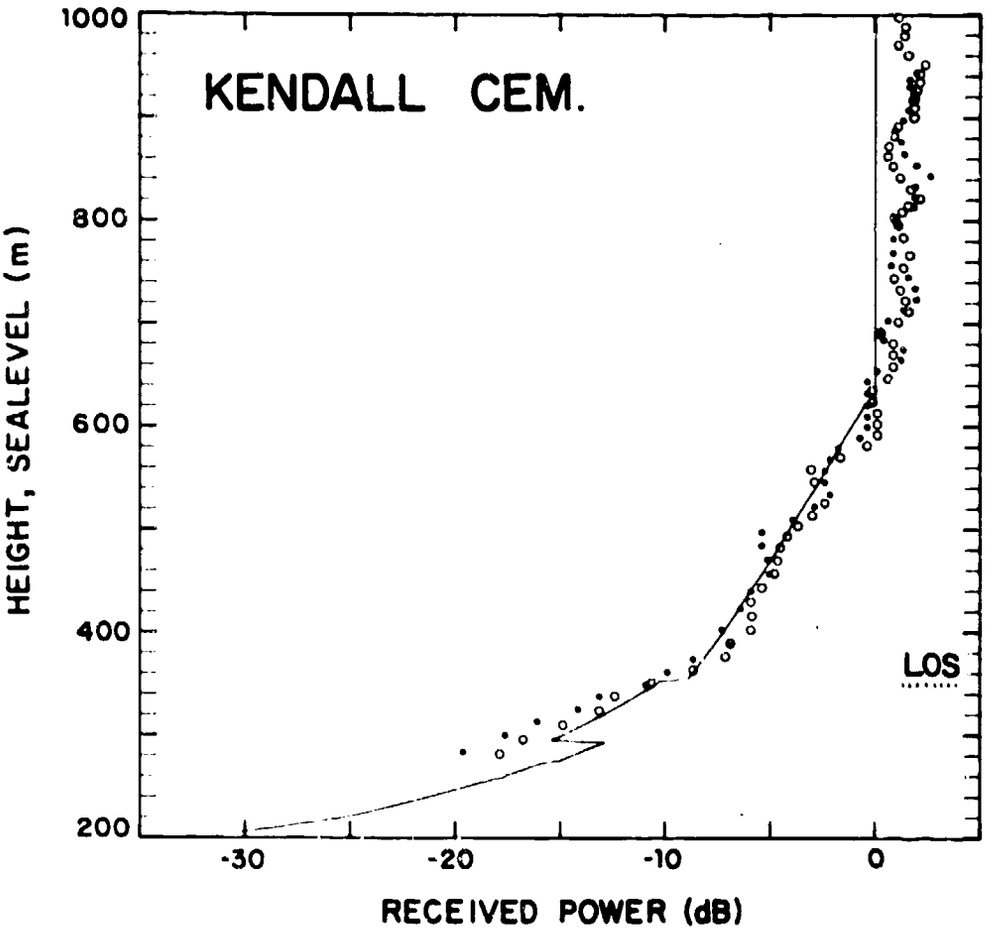

Fig. B-6 . Vertical-Probe Measurements and Predictions of the Longley-Rice Model at Kendall Cemetery.

agreement with the measurements, but for the other paths the agreement is poor. Table B-1 compares the RMS differences between model predictions and measurements for the Longley-Rice model and for the multiple-diffraction model. Note that RMS differences are slightly smaller for the Longley-Rice model than for the multiple-diffraction model on the Forest Hill and Kendall Cemetery paths, but on the other four paths the Longley-Rice model is significantly less accurate.

The complexity of the Longley-Rice model makes it difficult to determine why the performance should be so uneven. If we examine the profiles in Fig. 3, we can find no reason why the Longley-Rice predictions should be much more accurate for the Forest Hill and Kendall Cemetery paths than for the other paths. There are double knife-edges on the Forest Hill and Kendall Cemetery profiles, suggesting that the Longley-Rice model may be more accurate for double rather than single knife-edges. But the East Ware River path also crosses two prominent knife-edges, and the Longley-Rice predictions for this path are inaccurate, as Fig. B-3 shows. So this conjecture must be ruled out. We can conclude, however, that the overall performance of the multiple-diffraction model as indicated by Table B-1 is clearly superior to that of the Longley-Rice model.

TABLE B-1

COMPARISON OF PROPAGATION-MODEL PREDICTIONS:

LONGLEY-RICE MODEL VS. MULTIPLE-DIFFRACTION MODEL

Path Name	Quadrangle-Map Profiles RMS Difference (dB) Longley-Rice Model	Multiple Diffraction Model
Natty Pond	3.71	1.25
West Ware River	4.15	1.37
East Ware River	5.96	2.48
Forest Hill	1.68	1.72
Canesto Brook	4.42	2.44
Kendall Cemetery	1.32	2.09

ACKNOWLEDGMENTS

The author wishes to thank Dr. Roger W. Reed for many helpful discussions and for his assistance in programming the multiple-diffraction model and the computations of RMS difference between measurements and model predictions. The helicopter was flown through a series of difficult maneuvers with great skill by Mr. Thomas J. Magnan. The program for the multiple-diffraction model was written to the author's specifications by Ms. Janet W. Hazel, and the data were reduced with the help of Mr. Gerald L. McCaffrey, who programmed the data reduction, and Mr. Edward L. Philbrick, Jr., who transferred the data from the strip charts to the computer. Insight into the inner workings of the Longley-Rice model was provided by Dr. Robert E. Francois, Jr. We obtained our copy of the program for the Longley-Rice model from Dr. G. A. Hufford at the Institute for Telecommunications Studies, Boulder, Colorado, and he provided us with several sample computations that we used to validate this model on our computer.

REFERENCES

1. S. R. Anderson and R. B. Flint, "The CAA Doppler Omnirange," Proc. IEEE, 47, 808-821 (1959).

2. J. Deygout, "Multiple Knife-Edge Diffraction of Microwaves," IEEE Trans. Antennas Propag., AP-14, 611-620 (1966).

3. A. H. LaGrone, "Propagation of VHF and UHF Electromagnetic Waves over a Grove of Trees in Full Leaf," IEEE Trans. Antennas Propag., AP-25, 866-869 (1977).

4. A. G. Longley and P. L. Rice, "Predictions of Tropospheric Radio Transmission Loss over Irregular Terrain -- a Computer Method, 1968," Department of Commerce, ESSD Research Laboratories Report ERL 79-ITS 67, U. S. Government Printing Office, (1968). Modifications to this computer model were published as an Appendix to Department of Commerce, Office of Telecommunications Report 78-144 (April 1978).

5. M. L. Meeks, "A Propagation Experiment Combining Reflection and Diffraction," IEEE Trans. Antennas Propag. in press (1982). See also Project Report CMT-18, Lincoln Laboratory, Massachusetts Institute of Technology, Lexington, Massachusetts (26 October 1981) DTIC-AD-A108644.

6. G. Millington, R. Hewitt, and F. S. Immirzi, "Double Knife-Edge Diffraction in Field Strength Predictions," IEE, 109C, 419-429 (1962).

7. D. L. Sengupta, "Theory of V.O.R. Antenna Patterns," Electron. Lett., 7, 418-420 (1971).

8. S. O. Rice, "Diffraction of Plane Radio Waves by a Parabolic Cylinder," Bell Syst. Tech. J., 33, 417-504 (1954).

UNCLASSIFIED

SECURITY CLASSIFICATION OF THIS PAGE *(When Data Entered)*

REPORT DOCUMENTATION PAGE		READ INSTRUCTIONS BEFORE COMPLETING FORM
1. REPORT NUMBER ESD-TR-82-037	2. GOVT ACCESSION NO. AD-A115 776	3. RECIPIENT'S CATALOG NUMBER
4. TITLE *(and Subtitle)* VHF Propagation Over Hilly, Forested Terrain		5. TYPE OF REPORT & PERIOD COVERED Project Report
		6. PERFORMING ORG. REPORT NUMBER Project Report CMT-19
7. AUTHOR(s) M. Littleton Meeks		8. CONTRACT OR GRANT NUMBER(s) F19628-80-C-0002
9. PERFORMING ORGANIZATION NAME AND ADDRESS Lincoln Laboratory, M.I.T. P.O. Box 73 Lexington, MA 02173-0073		10. PROGRAM ELEMENT, PROJECT, TASK AREA & WORK UNIT NUMBERS Project No. 2E20 Program Element No. 62301E ARPA Order No. 3724
11. CONTROLLING OFFICE NAME AND ADDRESS Defense Advanced Research Projects Agency 1400 Wilson Boulevard Arlington, VA 22209		12. REPORT DATE 9 April 1982
		13. NUMBER OF PAGES 70
14. MONITORING AGENCY NAME & ADDRESS *(if different from Controlling Office)* Electronic Systems Division Hanscom AFB, MA 01731		15. SECURITY CLASS. *(of this report)* Unclassified
		15a. DECLASSIFICATION DOWNGRADING SCHEDULE

16. DISTRIBUTION STATEMENT *(of this Report)*

Approved for public release; distribution unlimited.

17. DISTRIBUTION STATEMENT *(of the abstract entered in Block 20, if different from Report)*

18. SUPPLEMENTARY NOTES

None

19. KEY WORDS *(Continue on reverse side if necessary and identify by block number)*

propagation measurements
propagation models
VHF propagation
computer model
knife-edge diffraction
multipath
forest

20. ABSTRACT *(Continue on reverse side if necessary and identify by block number)*

We have made propagation measurements at low altitudes over hilly, forested terrain with the objective of developing a computer-based propagation model capable of predicting path loss given the terrain profile between transmitter and receiver. The measurements were made at a frequency of 110.6 MHz with the VOR station at Gardner, Massachusetts, as a transmitter. The received signal was measured at distances between 7 and 15 km by making vertical descents with a helicopter from altitudes of roughly 806 m down to 10 m above ground. We found good agreement between the measurements and model predictions based on an extension of the Deygout approximation. Use of two knife-edges was sufficient to characterize the terrain diffraction. Negligible multipath reflection was observed from this terrain.

DD FORM 1 Jan 73 1473 EDITION OF 1 NOV 65 IS OBSOLETE

UNCLASSIFIED

SECURITY CLASSIFICATION OF THIS PAGE *(When Data Entered)*